CORONAVIRUS

Cytokinopathy with aberrant cytotoxic lymphocytes and profibrotic myeloid response in SARS-CoV-2 mRNA vaccine–associated myocarditis

Anis Barmada[1]†, Jon Klein[1]†, Anjali Ramaswamy[1]‡, Nina N. Brodsky[1,2]‡, Jillian R. Jaycox[1], Hassan Sheikha[1,2], Kate M. Jones[1], Victoria Habet[2], Melissa Campbell[2], Tomokazu S. Sumida[3], Amy Kontorovich[4], Dusan Bogunovic[4,5], Carlos R. Oliveira[2], Jeremy Steele[2], E. Kevin Hall[2], Mario Pena-Hernandez[1], Valter Monteiro[1], Carolina Lucas[1,6], Aaron M. Ring[1], Saad B. Omer[7,8,9], Akiko Iwasaki[1,6,10]*, Inci Yildirim[2,6,8,9]*, Carrie L. Lucas[1]*

Rare immune-mediated cardiac tissue inflammation can occur after vaccination, including after SARS-CoV-2 mRNA vaccines. However, the underlying immune cellular and molecular mechanisms driving this pathology remain poorly understood. Here, we investigated a cohort of patients who developed myocarditis and/or pericarditis with elevated troponin, B-type natriuretic peptide, and C-reactive protein levels as well as cardiac imaging abnormalities shortly after SARS-CoV-2 mRNA vaccination. Contrary to early hypotheses, patients did not demonstrate features of hypersensitivity myocarditis, nor did they have exaggerated SARS-CoV-2–specific or neutralizing antibody responses consistent with a hyperimmune humoral mechanism. We additionally found no evidence of cardiac-targeted autoantibodies. Instead, unbiased systematic immune serum profiling revealed elevations in circulating interleukins (IL-1β, IL-1RA, and IL-15), chemokines (CCL4, CXCL1, and CXCL10), and matrix metalloproteases (MMP1, MMP8, MMP9, and TIMP1). Subsequent deep immune profiling using single-cell RNA and repertoire sequencing of peripheral blood mononuclear cells during acute disease revealed expansion of activated CXCR3$^+$ cytotoxic T cells and NK cells, both phenotypically resembling cytokine-driven killer cells. In addition, patients displayed signatures of inflammatory and profibrotic CCR2$^+$ CD163$^+$ monocytes, coupled with elevated serum-soluble CD163, that may be linked to the late gadolinium enhancement on cardiac MRI, which can persist for months after vaccination. Together, our results demonstrate up-regulation in inflammatory cytokines and corresponding lymphocytes with tissue-damaging capabilities, suggesting a cytokine-dependent pathology, which may further be accompanied by myeloid cell–associated cardiac fibrosis. These findings likely rule out some previously proposed mechanisms of mRNA vaccine–-associated myopericarditis and point to new ones with relevance to vaccine development and clinical care.

INTRODUCTION

Vaccination against severe acute respiratory syndrome coronavirus 2 (SARS-CoV-2) is one of the most effective public health interventions in combating the ongoing coronavirus disease 2019 (COVID-19) pandemic. The SARS-CoV-2 spike mRNA vaccines have been found to be safe in international studies involving hundreds of thousands of individuals (*1*–*4*), although very rare cases of adverse events have been subsequently reported (*5*, *6*). One such adverse event is inflammation of the heart—namely, myocarditis, pericarditis, or a combination of the two (myopericarditis) (*7*–*12*). SARS-CoV-2 vaccine–associated myopericarditis has been reported to occur most frequently in adolescent and young adult males during the first week after the second dose of an mRNA vaccine (BNT162b2 or mRNA-1273) (*2*, *5*, *13*, *14*), although it can also occur across demographic groups after a single or third (booster) dose of mRNA vaccination or after non–mRNA-based vaccines (*5*, *15*–*19*). Various estimates of myopericarditis risk after vaccination have been reported (*2*, *7*, *14*, *17*, *20*–*23*), with most recent reports estimating an incidence of 0 to 35.9 and 0 to 10.9 cases per 100,000 for males and females, respectively, across age groups and mRNA vaccine cohorts (*24*). A study of vaccine-associated myopericarditis incidence from our own health care network (Yale New Haven Hospital) between January and May 2021 identified eight cases from 24,673 individuals aged 16 to 25 (0.3%) given two doses of mRNA vaccine (*25*).

Given the difficulties associated with studying such rare cases, the etiology of vaccine-associated myopericarditis remains largely unknown. A mechanistic understanding of the underlying pathology and associated immune alterations, as well as potential long-term effects, is needed and will likely have broad significance with the rapidly expanding clinical applications of effective mRNA-based vaccine modalities (*26*–*28*). Early hypotheses to explain

[1]Department of Immunobiology, Yale University School of Medicine, New Haven, CT, USA. [2]Department of Pediatrics, Yale University School of Medicine, New Haven, CT, USA. [3]Department of Neurology, Yale University School of Medicine, New Haven, CT, USA. [4]Zena and Michael A. Wiener Cardiovascular Institute, Mindich Child Health and Development Institute, Institute for Genomic Health, Icahn School of Medicine at Mount Sinai, New York, NY, USA. [5]Center for Inborn Errors of Immunity, Precision Immunology Institute, Mindich Child Health and Development Institute, Departments of Pediatrics and Microbiology, Icahn School of Medicine at Mount Sinai, New York, NY, USA. [6]Yale Center for Infection and Immunity, Yale University, New Haven, CT, USA. [7]Department of Medicine, Yale University School of Medicine, New Haven, CT, USA. [8]Epidemiology of Microbial Diseases, Yale School of Public Health, New Haven, CT, USA. [9]Yale Institute for Global Health, Yale University, New Haven, CT, USA. [10]Howard Hughes Medical Institute, Chevy Chase, MD, USA.
*Corresponding author. Email: carrie.lucas@yale.edu (C.L.L.); inci.yildirim@yale.edu (I.Y.); akiko.iwasaki@yale.edu (A.I.)
†These authors contributed equally to this work.
‡These authors contributed equally to this work.

mRNA vaccine–associated myopericarditis speculated that the SARS-CoV-2 spike protein, which may be detectable in the blood (*29*) and sparsely on cardiomyocytes (*30*) of patients in some studies, may induce cardiac-targeted autoantibodies through molecular mimicry, although this has so far not been supported by other reports (*31*, *32*). Alternative hypotheses suggested that hypersensitivity myocarditis may instead explain the pathology, primarily based on clinical presentation, rapid recovery, and marked increase in incidence after second doses of mRNA vaccines (*11*, *33*). However, early case reports and cardiac biopsies from small numbers of patients were largely inconsistent with such a pathology (*9*, *34*–*36*). Biopsy reports showed an inflammatory infiltrate predominantly composed of macrophages and T lymphocytes, although scattered eosinophils, B cells, and plasma cells were additionally noted in some reports (*37*). Autoimmune myocarditis driven by T helper type 17 (T_H17) responses is another possible mechanism (*38*, *39*), although no evidence supporting such a pathology was found in the limited number of patients profiled to date (*32*, *40*). Other arguments proposed aberrant immune reactivity, both innate and adaptive, triggered by the mRNA and/or lipid nanoparticles (LNPs) (*13*, *41*, *42*). Further, recent studies in two patients implicated a role for various inflammatory cytokines as well as natural killer (NK) and T lymphocytes (*32*, *40*). Each of these proposed mechanisms can be influenced by age, sex, and genetic background, leading to increased incidence in certain subpopulations (*13*). To better understand the underlying pathology in SARS-CoV-2 LNP-mRNA vaccine–associated myopericarditis, we conducted a multimodal study of patients with acute myocarditis and/or pericarditis using unbiased approaches that define the maladaptive immune signatures during disease.

RESULTS

Vaccine-associated myopericarditis patient cohort and clinical presentation

Our clinical cohort consists of 23 patients with vaccine-associated myocarditis and/or pericarditis. The cohort was predominately male (87%) with an average age of 16.9 ± 2.2 years (ranging from 13 to 21 years), in congruence with prior epidemiological reports (*24*). Patients had largely noncontributory past medical histories and were generally healthy before vaccination. Most patients had symptom onset 1 to 4 days after the second dose of the BNT162b2 mRNA vaccine (Fig. 1A and tables S1 and S2). Six patients either first experienced symptoms after a delay of >7 days after vaccination (P18, P20, P22, and P23) or were incidentally positive for SARS-CoV-2 by polymerase chain reaction (PCR) testing upon hospital admission (P19 and P21) (fig. S1A); these six patients were thus excluded from further analyses, although they potentially reflect the breadth of clinical presentations of vaccine-associated myopericarditis. Our remaining cohort of patients showed no evidence of recent prior SARS-CoV-2 infection, with antibodies to spike (S) protein but not to nucleocapsid (N) protein and negative nasopharyngeal swab reverse transcription quantitative PCR at hospital admission.

Symptom presentation was consistent with acute myocarditis and/or pericarditis, including chest pain, palpitations, fever, shortness of breath, headaches, myalgia, diaphoresis, fatigue, nausea/emesis, and/or congestion (table S1). Laboratory testing in most patients during hospital admission demonstrated elevations in the maximum observed levels of troponin, C-reactive protein (CRP), and B-type natriuretic peptide (BNP) (Fig. 1, B to D and table S1), indicating acute systemic inflammation with direct myocardial injury. Some patients also had leukocytosis (Fig. 1E; for complete blood count differential, see fig. S1, C to K) and elevated neutrophil-to-lymphocyte ratio (NLR) (Fig. 1F), consistent with systemic inflammation. Levels of eosinophils and basophils were within normal limits (fig. S1, F and G).

Electrocardiogram (ECG) performed at admission revealed abnormal findings ranging from nonspecific abnormalities to ST segment elevations and PR segment depressions consistent with pericarditis (table S1). Echocardiogram findings demonstrated borderline low or abnormally reduced left ventricle ejection fraction in several patients, consistent with the diagnosis of myocarditis and/or pericarditis. Most patients further underwent cardiac magnetic resonance (CMR) imaging during acute hospitalization, revealing imaging abnormalities consistent with acute or subacute myocarditis and/or pericarditis (table S1 and fig. S1B).

Patients were treated with nonsteroidal anti-inflammatory drugs, and some also received steroids and intravenous immunoglobulin (Fig. 1A and fig. S1A). Patients were discharged home with improving symptoms and clinical laboratory findings after 1 to 6 days. Although patients showed rapid resolution of clinical symptoms with improved laboratory findings, most of them maintained some imaging abnormalities. These included late gadolinium enhancement (LGE) at longitudinal clinical follow-up at least 2 months after hospital discharge, as assessed by CMR (table S1).

Lack of evidence for potentially pathogenic antibodies in myopericarditis

To first assess whether patients with myopericarditis generate overexuberant humoral responses to vaccination, we performed enzyme-linked immunosorbent assays (ELISAs) for SARS-CoV-2–specific S, S1 subunit, and receptor binding domain (RBD) antibodies. Compared with healthy vaccinated controls (VCs, $n = 16$), including those closer in age to patients where there is an increased risk for vaccine-associated myopericarditis [younger VCs (YVC), $n = 6$], patients with myopericarditis ($n = 9$) had no evidence of enhanced anti–SARS-CoV-2 antibodies (fig. S2, A to C). Given the rather moderately reduced levels of SARS-CoV-2–specific antibodies observed in the patients, we next investigated whether the development of myopericarditis was associated with blunted generation of neutralizing antibody responses in these patients. We performed plaque reduction neutralization tests ($PRNT_{50}$) and found a reduction in the estimated 50% serum inhibitory concentration (IC_{50}) between patients and healthy VCs with no prior history of SARS-CoV-2 exposure (Fig. 2A), possibly owing to the differences in sample collection time relative to vaccination (3 to 11 days for patients versus 7 days for controls). These results suggest that patients with myopericarditis do not display enhanced SARS-CoV-2–specific and neutralizing antibody responses at the time of acute disease presentation but rather show comparable or potentially blunted responses compared to healthy VCs.

To further interrogate whether patients with myopericarditis generate self-targeted autoantibodies after vaccination, we used rapid extracellular antigen profiling (REAP) to screen patients' plasma for autoantibodies, as has been previously validated (*43*, *44*). In total, autoantibodies recognizing 6183 different human extracellular or secreted proteins/epitopes were assessed by REAP. Of

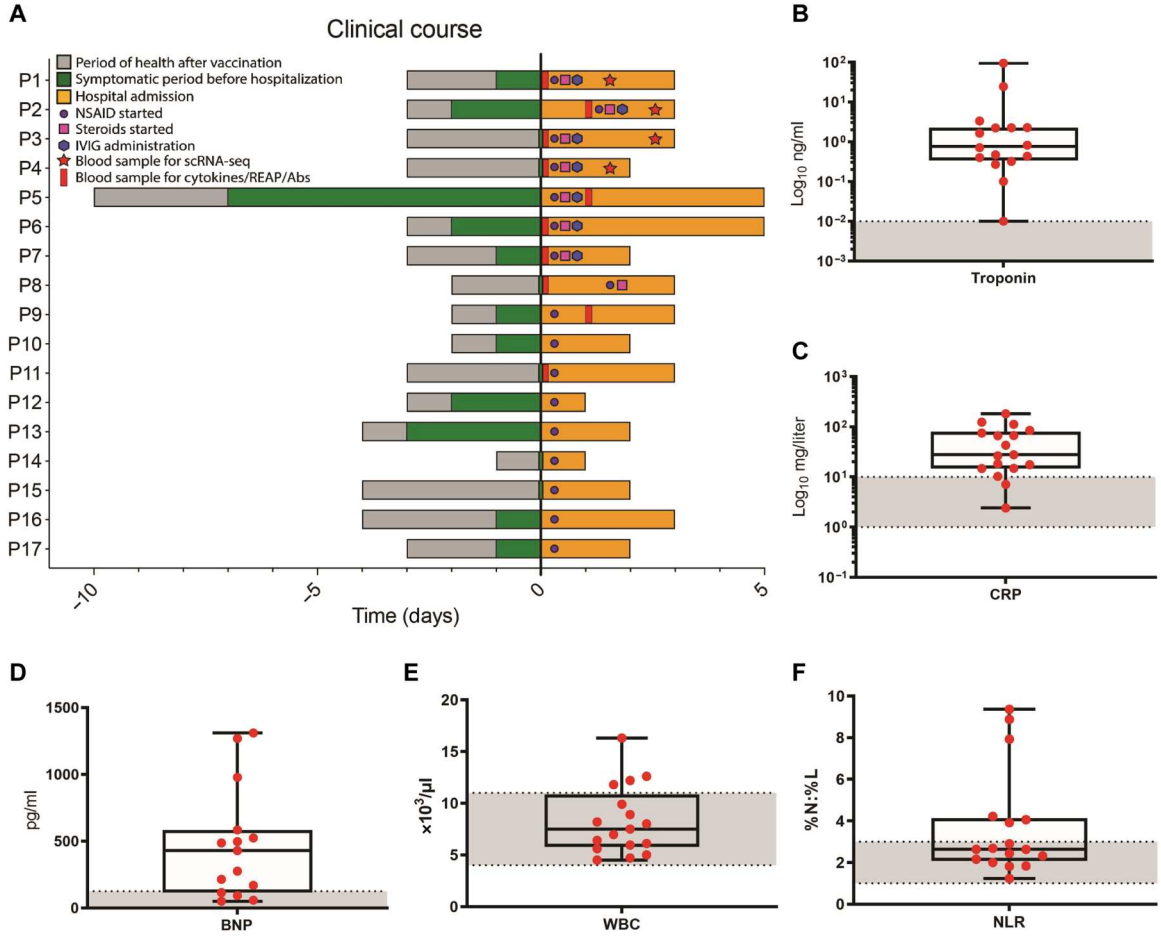

Fig. 1. Clinical parameters of the SARS-CoV-2 vaccine–associated myopericarditis cohort. (**A**) Time course for patients showing the day of vaccine administration, symptom onset, treatment, and sample collection relative to hospital admission (day 0). (**B** to **F**) Maximum values of selected blood markers in patients tested during hospital admission. Boxes depict the interquartile range (IQR), horizontal bars represent the median, whiskers extend to 1.5 × IQR, and red dots show the value of each patient. Dashed lines and gray area represent normal reference ranges used at Yale New Haven Hospital. CRP, C-reactive protein; BNP, B-type natriuretic peptide; WBC, white blood cell; NLR, neutrophil-to-lymphocyte ratio; REAP, rapid extracellular antigen profiling; Abs, antibodies; IVIG, intravenous immunoglobulin; NSAID, nonsteroidal anti-inflammatory drug.

these, we focused on 526 antigens/epitopes relevant to cardiac function, defined either as members of the Gene Ontology (GO) terms "circulatory system process" or "heart contraction" or as "heart tissue enriched/enhanced" in the Human Protein Atlas. Our analysis showed no elevation in the frequency of targeting autoantibodies in patients with myopericarditis compared to YVCs (Fig. 2B and fig. S2D). REAP applied to a separate control cohort of hospitalized patients with COVID-19 ($n = 60$) showed positive signals for several of these cardiac-related autoantibodies, demonstrating the ability to detect such autoantibodies when present (fig. S2E).

Cytokinopathy revealed by unbiased analysis of serum proteins and immune cell subsets in myopericarditis

Having found no evidence to support hypersensitivity myocarditis or antibody-mediated processes, we next sought to take a broad and unbiased approach to uncover immune changes in patients with myopericarditis during acute disease. To this end, we first performed serum protein profiling in patients ($n = 9$) and healthy YVCs ($n = 6$). Analysis of circulating inflammatory mediators in myopericarditis revealed elevations [false discovery rate (FDR) < 0.05] of the interleukin-1 (IL-1) family cytokines (IL-1β and IL-1RA) (Fig. 3A), consistent with earlier clinical findings suggesting acute, systemic inflammation. In addition, the cytokine IL-15, which can activate NK and T cells, was elevated in myopericarditis. Increases in lymphocyte- and monocyte-directed chemokines were also observed (CCL4, CXCL1, and CXCL10) (Fig. 3A). Given the inflammatory profile and cardiac injury observed in patients with myopericarditis, we also explored levels of matrix metalloproteases and corresponding counter-regulatory proteins and found that they were also elevated [matrix metalloproteinase 1 (MMP1), MMP8, MMP9, and tissue inhibitor of matrix metalloproteinase 1 (TIMP1)]. We next performed exploratory principal components analysis (PCA) involving all measured proteins/cytokines (84 total from Fig. 3A and fig. S3) to identify whether distinct disease immune phenotypes exist among the patients and compared with healthy YVCs. Groups separated well [principal component 1 (PC1): 47.44% of variance], indicating clear differences in immune phenotypes and suggesting ongoing cytokinopathy in

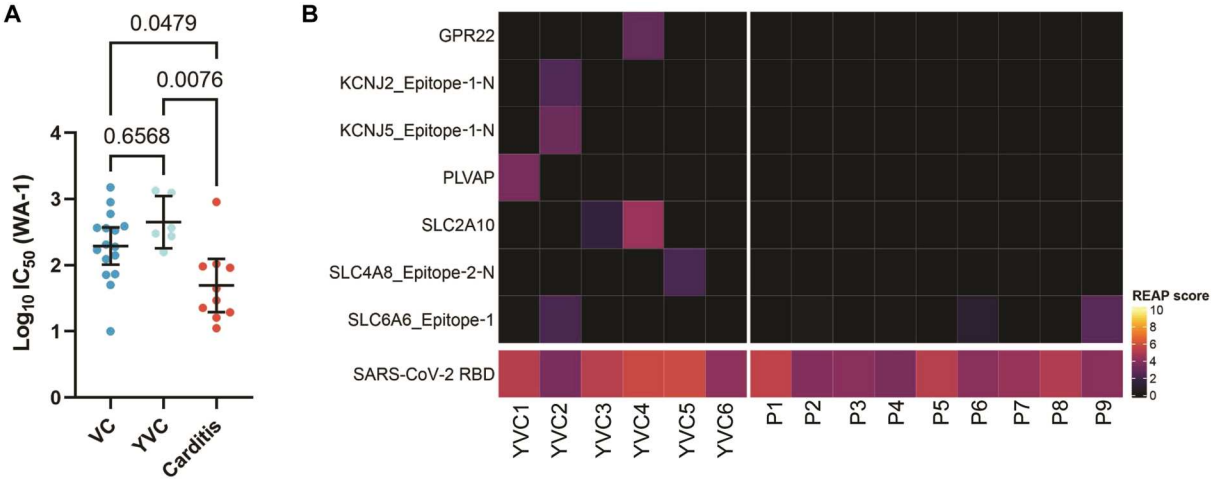

Fig. 2. Myopericarditis patients mount humoral response to vaccination with no evidence of reactive autoantibodies. (**A**) IC_{50} estimates for SARS-CoV-2 neutralizing antibody titers against ancestral SARS-CoV-2 (WA-1) in patients ($n = 10$) compared with healthy VCs ($n = 16$), in addition to those closer in age to patients where there is an increased risk for vaccine-associated myopericarditis (YVCs, $n = 6$). Black bars denote group means, and error bars represent 95% confidence intervals. Statistical significance was assessed using the Kruskal-Wallis test with Dunn's correction for multiple comparisons. (**B**) Heatmap of REAP scores showing cardiac-related autoantibodies present in at least one donor (either patients or YVCs), from a total of 526 antigens/epitopes defined by GO (circulatory system process (GO:0003013) or heart contraction (GO:0060047) or the Human Protein Atlas (heart tissue enriched/enhanced), across individual patients ($n = 9$) and YVCs ($n = 6$). SARS-CoV-2 RBD antigen was used as a positive control in vaccinated individuals. Positive autoantibody reactivity is defined as REAP score ≥ 2, protein-wise z score ≥ 1.96, and protein-wise mean < 0.5, where higher REAP scores correlate with higher antibody titer and/or abundance as validated previously (*43*, *44*). Negative findings for all cardiac antigens/epitopes tested from the Human Protein Atlas (81 total) are further shown in fig. S2D.

patients with myopericarditis (Fig. 3B and fig. S4, A to D). Patients additionally appeared to separate into two groups (PC2: 21.50% of variance), where one was characterized by MMPs, including MMP1 and MMP8 (Fig. 3B and fig. S4, A and B). Upon CMR imaging, patients in this group (P1, P3, P6, and P9) displayed LGE at presentation, whereas the patient in the other group (P2) had no LGE (table S1).

Complementing our serum analysis, we performed single-cell RNA sequencing (scRNA-seq) on peripheral blood mononuclear cells (PBMCs) of the four patients (P1 to P4) from whom suitable samples could be collected during acute illness to better define and correlate the immune effectors in vaccine-associated myopericarditis. Because inflammatory effects from vaccination may be transient, we integrated these samples with ones from healthy young male donors matched for time after vaccination [early-young vaccinated controls (E-YVCs), $n = 4$]. These controls received the third (booster) dose of mRNA vaccine, which has been reported to induce greater inflammatory side effects compared with the second dose (*17*, *45*), thus controlling for the benign inflammation early after vaccination in young adult males to help separate the likely pathological signatures in myopericarditis. We additionally included samples from three of the patients at follow-up/recovery (R-P1 191 days, R-P3 195 days, and R-P4 190 days after vaccination), four samples from pediatric male healthy donor (HD) controls, and four samples from multisystem inflammatory syndrome in children (MIS-C) patients after SARS-CoV-2 were analyzed using cellular indexing of transcriptomes and epitopes by sequencing [CITE-seq; (*46*)] to enable refined annotation of cell subsets using surface protein markers (Fig. 3C and tables S2 and S3). After quality control and processing, we obtained a total of 221,727 cells segregating into 44 distinct cell clusters, including unique subsets of myeloid, NK, B, and T cells (Fig. 3D and fig. S5, A to D). We observed the presence of plasma B cells and dividing plasmablasts in patients with myopericarditis (fig. S6, A and B), which was further validated using flow cytometry (fig. S6C). To further evaluate whether these B cells had features of autoantigen-reactive responses, we performed B cell receptor (BCR) repertoire analysis. We observed no significant reduction in clonal diversity or increase in the proportion of immunoglobulin G (IgG) clones harboring mutated BCR regions (fig. S6, D and E), providing little evidence for clonal expansion or somatic hypermutation and supporting findings from our earlier neutralizing antibody and REAP analyses. Differences were observed in the isotype distribution and proportion of cells expressing IgG1 or IgG3 between myopericarditis and healthy E-YVCs, although these did not reach statistical significance (fig. S6, F to I). Overall, these findings potentially suggest nonspecific expansion of plasma B cells and plasmablasts because of the broad cytokinopathy and/or secondary responses to systemic inflammation in these patients.

NK cell dysregulation in myopericarditis

Given the cytokinopathy in myopericarditis and specifically the elevation of IL-15 observed in our serum analysis, we first investigated changes in NK cell subsets. The elevation of IL-15 was validated in our scRNA-seq cohort using ELISA (fig. S7A). In addition, we noted increased proportions of a $CD16^+$ NK cell subset ($P = 0.087$ after correction for multiple comparisons) in patients (fig. S7B). This trend was not mirrored in innate-like T cells, including Vδ2 γδ T and mucosal-associated invariant T (MAIT) cells (fig. S7, C and D), possibly indicating unique effects in NK cells. To further investigate whether this NK subset is up-regulating genes downstream of the activating cytokine IL-15, we made use of a published gene set of the *IL2RB* pathway (GSEA Molecular Signatures Database (MSigDB) M8615) and saw up-regulation of various genes

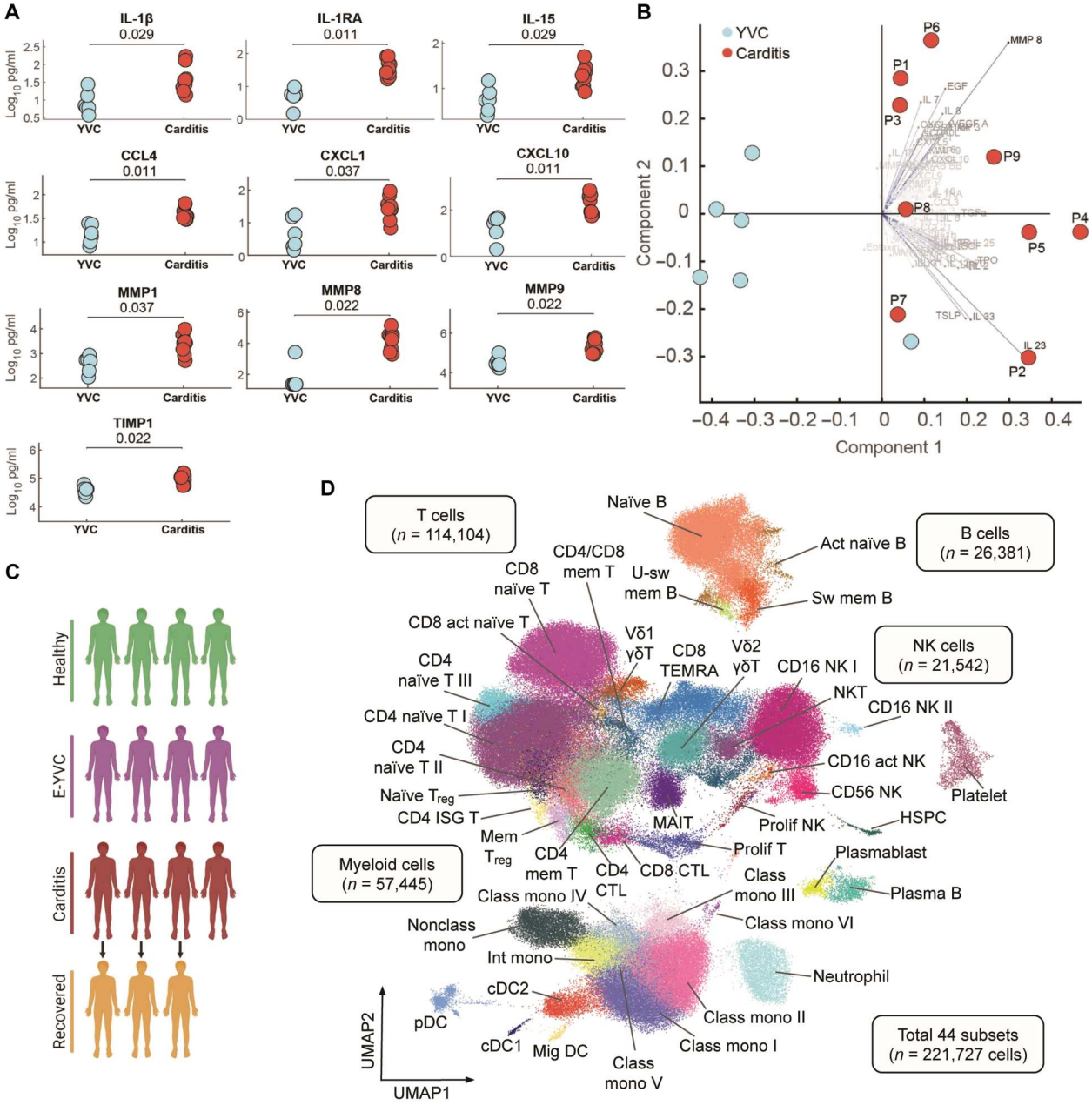

Fig. 3. Elevation of immune cytokines in myopericarditis and identification of immune cell subsets. (**A**) Scatter plots of selected cytokines in patients ($n = 9$) and healthy YVCs ($n = 6$). Statistical significance was determined using the unpaired two-sided Wilcoxon rank-sum test with Benjamini-Hochberg FDR correction for multiple comparisons. All additional serum proteins assayed are shown in fig. S3. (**B**) Biplot of all serum proteins assayed (84 total) between patients and healthy YVCs (see related PCA in fig. S4, A and B). (**C**) Schematic diagram showing the cohort studied in subsequent scRNA-seq analyses, including pediatric male HDs ($n = 4$), healthy E-YVCs ($n = 4$), patients with acute myopericarditis ($n = 4$), and matched patients at follow-up/recovery ($n = 3$). (**D**) UMAP visualization of immune cell subsets identified from the cohort in (C), with additional four CITE-seq samples from patients with MIS-C after SARS-CoV-2 included to refine cluster annotation using surface proteins. act, activated; sw, class-switched; u-sw, class-unswitched; mem, memory; NK, natural killer cell; NK T, natural killer T cell ($CD3^+$ $CD161^+$ $KLRF1^+$); T_{reg}, regulatory T; ISG, IFN-stimulated gene; CTL, cytotoxic T lymphocyte; prolif, proliferating; MAIT, mucosal-associated invariant T; TEMRA, terminally differentiated effector memory $CD45RA^+$ T; nonclass, nonclassical; int, intermediate; class, classical; mono, monocyte; cDC, conventional dendritic cell; pDC, plasmacytoid dendritic cell; mig, migratory; HSPC, hematopoietic stem and progenitor cell.

(FDR < 0.05), including both the *IL2RG* and *IL2RB* subunits of the IL-15 receptor (fig. S7E). To better define the transcriptional signature in this subset, we used differential gene expression in comparison with the rest of the CD16$^+$ NK cells. Top up-regulated genes included NK receptors, including the activating receptor NKG2D (or *KLRK1*) that recognizes stress-induced cell surface ligands, cytotoxicity-related genes (*GZMA* and *PRF1*), degranulation and activation markers (*LAMP1*, *LAMP2*, and *CD69*), as well as various integrins and chemokines, among others (fig. S7F). Top down-regulated genes notably included various alarmins (*S100A4*, *S100A6*, *S100A10*, and *S100A11*) and interferon (IFN)–stimulated genes (*ISG15*, *ISG20*, *LY6E*, *IFITM1*, *IFITM3*, and *IFITM2*), which may be associated with subset-specific dysregulated NK cell signaling, because this gene expression pattern was not reflected across other cell types. Similarly, consistent with the known internalization of NKG2D after ligand engagement, which acts as potential negative feedback to desensitize NK cell responses (*47*, *48*), we observed significantly reduced levels of NKG2D protein on the surface of NK cells in patients by flow cytometry (fig. S7G). One hypothesis is that these parallel analyses of transcripts and surface protein for NKG2D potentially reflect recent NK cell cytotoxic engagement, consistent with their capacity to mediate tissue damage. Overall, we describe a signature of NK cell dysregulation and activation, which may be linked to the development of vaccine-associated myopericarditis.

Expansion of activated cytotoxic T lymphocytes in myopericarditis

Next, to inspect changes in the proportions of T cell subsets across the groups while accounting for compositional dependencies between the subsets, we used the Bayesian model scCODA (myopericarditis versus E-YVCs, FDR < 0.05) (*49*). We observed significantly decreased proportions of a CD4$^+$ naïve T cell subset paired with robust expansions of cytotoxic T lymphocytes (CTLs), both CD4$^+$ and CD8$^+$, and proliferating T cells in myopericarditis (Fig. 4, A to D). Upon examining the transcriptional signature of these expanded subsets, we noted the unique expression of various activation markers, including programmed cell death protein-1 (PD-1) (*PDCD1*) and CD38/HLA-DR (Fig. 4E), which was further validated by flow cytometry in CD8$^+$ T cells (Fig. 4F). These CTLs and proliferating T cells further expressed the chemokine receptors CXCR3 and CCR5 (Fig. 4E), whose ligands —CXCL10 and CCL4, respectively—were shown to be significantly elevated in our earlier serum analysis of the patient cohort (Fig. 3A). These chemokines are known to play central roles in recruitment of T cells to heart tissue, leading to cardiac infiltration of proinflammatory CTLs, and they have previously been described in the context of various inflammatory cardiovascular diseases, including classic myocarditis (*50*–*58*). Moreover, these cell subsets express perforin (*PRF1*) and a diverse set of granzymes (including *GZMA*, *GZMB*, *GZMH*, and *GZMK*), equipping them to be tissue damaging (Fig. 4E). Further, CD8$^+$ T cells in patients showed significantly increased phosphorylated signal transducers and activators of transcription 3 (STAT3) (pSTAT3), indicating ongoing cytokine sensing, compared with E-YVCs by flow cytometry (Fig. 4G). In contrast, published studies of healthy vaccinated donors showed maximum elevation in pSTAT3 1 day after mRNA secondary vaccination (*59*). To test the hypothesis that these cells are similar to heart CTLs, we trained a logistic regression model using published single-cell data of heart T cells (*60*) to predict concordant cell subsets in our dataset on the basis of gene expression. Although multiple cell subsets mapped to heart CD4$^+$ effector-memory T (CD4$^+$ T_tem) cells (suggesting that these cells are most transcriptionally similar to blood circulating T cells) and others did not map well to any single heart population (likely due to tissue adaptability or disease-specific signatures), CD8$^+$ CTLs mapped with high frequency to the corresponding heart subset (Fig. 4H), potentially suggesting similarities beyond the cytotoxicity profile.

In addition, to assess the possibility of clonal expansion in these dysregulated T cell subsets, we analyzed the T cell receptor (TCR) repertoire of patients with myopericarditis. An assessment of repertoire diversity, as measured by richness and evenness (Shannon index/richness), revealed that non-naïve CD4$^+$ and CD8$^+$ T cells were highly diverse across cohorts (fig. S8A). Although CTLs and proliferating T cells were expanded in patients (Fig. 4, B to D), we did not see significant changes in the Vβ usage and found little evidence of highly expanded clones in these cells (fig. S8, B and C), although the possibility of autoreactive cells cannot be fully excluded. Of note, patients with myopericarditis did not display an expansion of *TRBV11-2*$^+$ pathogenic T cells as seen in SARS-CoV-2–associated MIS-C (fig. S8D) (*61*–*64*). In summary, T cells in myopericarditis bear an activated signature despite having comparable diversity to healthy VCs, consistent with a cytokine-dependent activation of CTLs after vaccination.

Monocyte dysregulation with evidence of cardiac fibrosis in myopericarditis

With the extensive inflammatory profile observed in myopericarditis and signs of cardiac injury and LGE on CMR imaging, we lastly investigated changes in the innate myeloid compartment. Compositional analysis (scCODA, FDR < 0.05) revealed a significant decrease in CD14^{dim} CD16$^+$ nonclassical monocytes, which are commonly anti-inflammatory (*65*, *66*), paired with an increase in inflammatory CD14$^+$ CD16$^-$ classical monocytes (Fig. 5, A and B). These classical monocytes further showed increased expression of genes from the S100A family of alarmins in myopericarditis (Fig. 5C), supporting their role in the inflammatory response and consistent with the elevations we saw in IL-1β (*39*, *67*, *68*). Such classical monocytes can further differentiate into tissue macrophages and contribute to chronic disease (*65*). To better define this possibility in myopericarditis, we used a published dataset of 238 genes (GSEA MSigDB M3468) encoding enzymes/proteins and regulators involved in extracellular matrix remodeling. We observed an up-regulation of this remodeling and profibrotic signature in classical monocytes of patients with myopericarditis (Fig. 5D), consistent with our earlier serum protein/enzyme analysis in these patients (Fig. 3A). In addition, we performed differential gene expression analysis (FDR < 0.05, logFC >0.1), revealing the up-regulation of various specific genes shared across patients (Fig. 5E). These genes included *CD163*, which marks tissue-resident macrophages (*69*) and has been associated with a profibrotic phenotype (*70*). Positive CD163 immunostaining was previously reported on myocardial inflammatory infiltrates in myocarditis after COVID-19 (*71*, *72*) and adenovirus-vectored (Ad26.COV2.S) SARS-CoV-2 vaccination (*73*). These monocytes also expressed *CCR2* (Fig. 5E), which enables migration to sites of tissue injury and differentiation into inflammatory cardiac macrophages, including in myocarditis

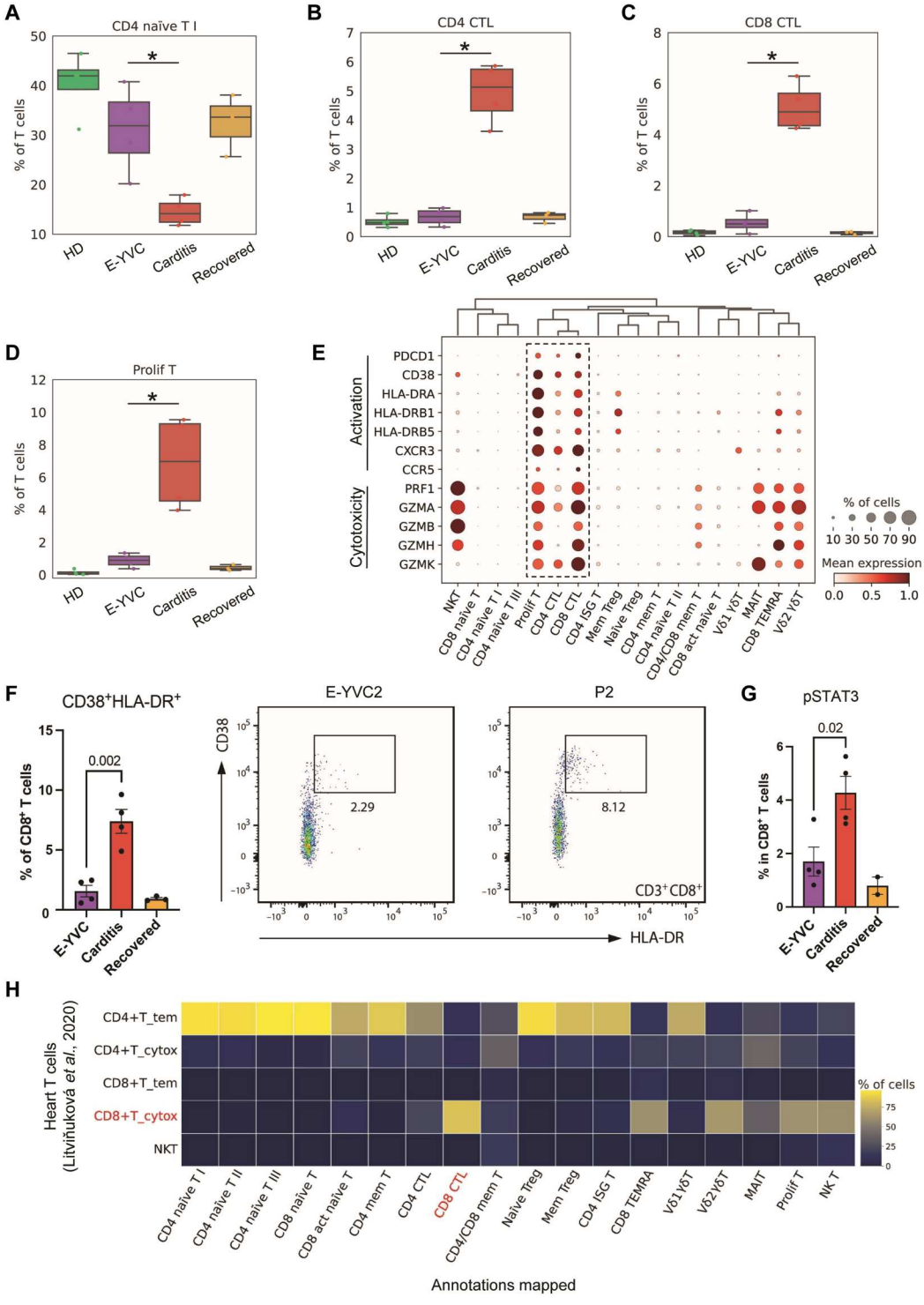

Fig. 4. Expansion of activated CTLs in myopericarditis. (**A** to **D**) Box plots showing the average proportions of four T cell subsets ($CD4^+$ naïve T I, $CD4^+$ and $CD8^+$ CTLs, as well as proliferating T cells) across the groups. The boxes denote the IQR, horizontal bars represent the median, whiskers extend to 1.5 × IQR, and dots show the values of each donor. Statistical significance was determined using the Bayesian model scCODA (*49*) accounting for the compositional dependencies between cell subsets in the scRNA-seq data while controlling for false discoveries (FDR < 0.05 in myopericarditis versus E-YVCs). (**E**) Dot plot showing the expression of activation markers (PD-1 and CD38/HLA-DR), chemokine receptors (*CXCR3* and *CCR5*), and cytotoxicity genes (perforin and granzymes) characterizing the T cell subsets shown in (B to D). (**F**) Flow cytometry quantifying the percentage of the $CD38^+$ $HLA\text{-}DR^+$ population out of $CD8^+$ T cells across the groups (left), with representative plots for E-YVCs and patient (P2) donors (right). Statistical significance was determined using the unpaired two-tailed *t* test between the E-YVC and myopericarditis groups, and error bars represent the SE. (**G**) Percentage pSTAT3 in $CD8^+$ T cells across the groups by flow cytometry; statistical significance was determined as in (F), and error bars represent SE. (**H**) Heatmap depicting the percentage of each T cell subset identified in this study that mapped, using a logistic regression model based on gene expression with mean prediction probability of 0.9, to each subset from published single-cell data of heart T cell populations (*60*).

(*66*, *74*–*76*). The abundance of $CCR2^+$ macrophages has been associated with cardiac remodeling and fibrosis (*74*, *77*). These results are in agreement with the elevations in various MMPs shown by our earlier serum analysis of the patient cohort (Fig. 3A). Other up-regulated genes included ones involved in procollagen processing (*ADAMTS2*), adhesion and migration (*ITGAM*, also known as MAC-1 or CD11b), as well as likely inflammation and oxidative stress (*CLEC4E*, *RNASE2*, *FKBP5*, *GSR*, *MARC1*, and *SULT1A1*) (Fig. 5E). Upon monocyte/macrophage activation, CD163 is shed from the cell surface, and its serum levels can be further associated with fibrosis (*78*, *79*). In our patients, soluble CD163 (sCD163) was confirmed to be significantly elevated in serum (Fig. 5F). Together, our findings potentially provide a mechanistic link to the LGE findings in the majority of patients in our cohort (Fig. 5G), which can

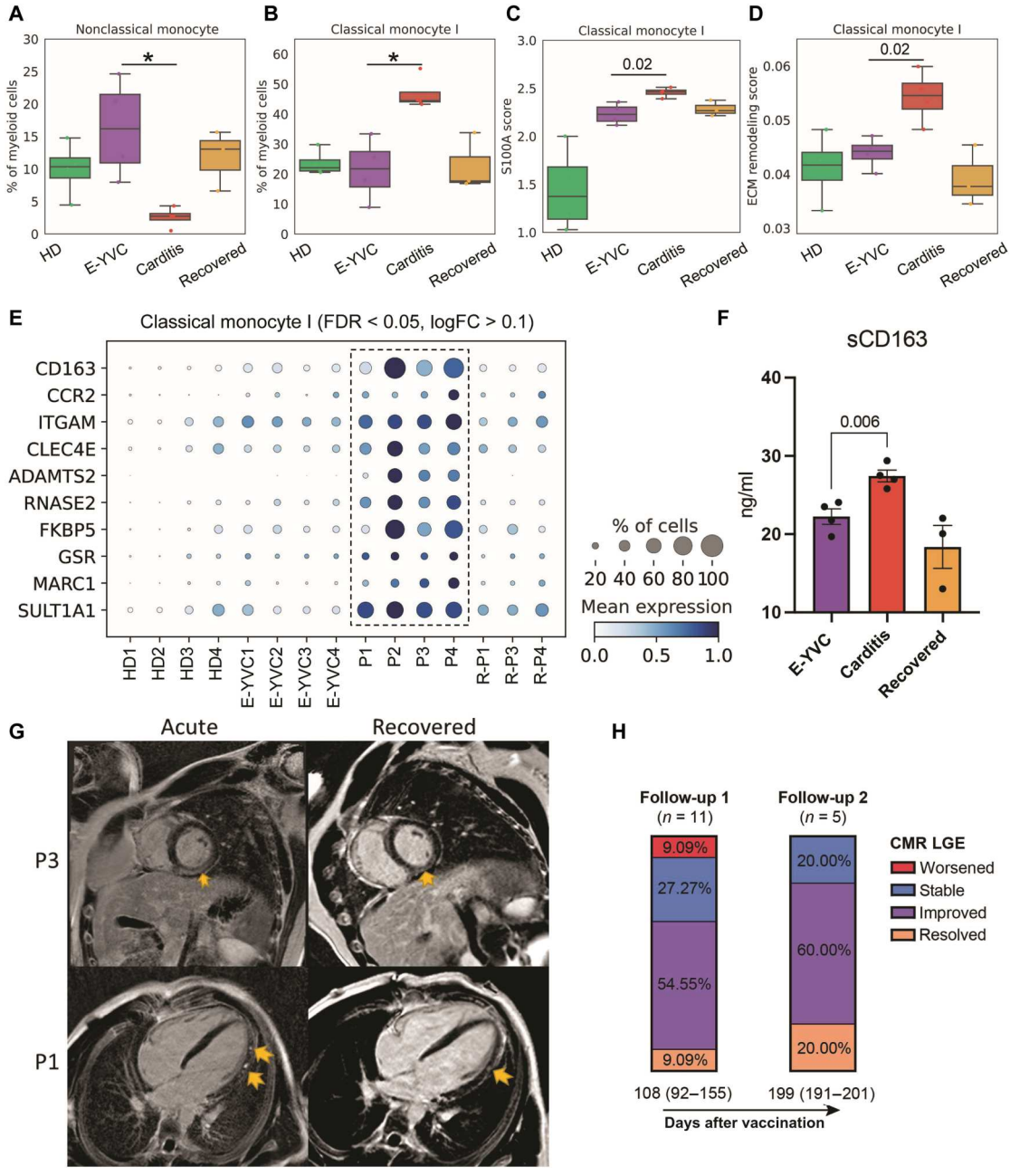

Fig. 5. Inflammatory and profibrotic signatures of monocytes in myopericarditis. (**A** and **B**) Box plots showing the average proportions of nonclassical ($CD14^{dim}$ $CD16^{+}$) and classical ($CD14^{+}$ $CD16^{-}$) monocyte subsets across the groups. The boxes denote the IQR, horizontal bars represent the median, whiskers extend to 1.5 × IQR, and dots show the values of each donor. Statistical significance was determined using the Bayesian model scCODA (*49*) accounting for the compositional dependencies between cell subsets in the scRNA-seq data while controlling for false discoveries (FDR < 0.05 in myopericarditis versus E-YVCs). (**C** and **D**) Average expression score of (C) inflammatory genes from the S100A family of alarmins (*S100A8-12*; FDR < 0.05, logFC > 0.1 in myopericarditis versus E-YVCs) and (D) 238 genes from a published dataset of extracellular matrix (ECM) remodeling (GSEA MSigDB M3468) in the same classical monocyte subset shown in (B) across groups. Statistical significance between scores was determined using the unpaired two-sided Wilcoxon rank-sum test comparing the E-YVC and myopericarditis groups. (**E**) Dot plot showing top differentially expressed and up-regulated genes in the same classical monocyte subset shown in (B) across donors (FDR < 0.05, logFC > 0.1 in myopericarditis versus E-YVCs). (**F**) ELISA measurement of sCD163 in serum across the groups. Statistical significance was determined using the unpaired two-tailed *t* test between the E-YVC and myopericarditis groups, and error bars represent the SE. (**G**) Representative CMR images of acute myopericarditis and follow-up/recovery (191 days for P1 and 82 days for P3 after vaccination) showing persistent LGE (yellow arrows) seen in a subset of patients (from 17 patients included in our cohort, at admission, 11 were LGE positive, 4 were LGE negative, and 2 had no CMR). Particularly, for P1, four-chamber phase sequence inversion recovery (PSIR) demonstrating patch subepicardial LGE along the left ventricular lateral wall from base to apex (acute), with improvement in both quantity and intensity at follow-up (recovered). For P3, mid-ventricle short axis PSIR demonstrating subepicardial to nearly transmural LGE sparing the subendocardial region (acute), which was mildly improved in intensity and quantity at follow-up (recovered). (**H**) Stacked bar plots depicting the percentage of patients categorized by CMR LGE changes at two follow-ups after vaccination/first admission [median days (IQR)]. Additional details of imaging findings and patients with LGE at admission and follow-up are in table S1.

persist for months after vaccination (Fig. 5H). These results may further suggest the need for careful long-term monitoring of patients with myocarditis and/or pericarditis exhibiting signs of cardiac fibrosis. In summary, our results point to the effector immune populations in vaccine-associated myopericarditis, consistent with published biopsy reports demonstrating a predominate macrophage and lymphocytic immune infiltrate of affected heart tissue (*30*, *34*–*37*, *80*).

DISCUSSION

Although rare, vaccine-associated myopericarditis has emerged as an important area of investigation with implications for scientists and physicians working to optimize vaccination strategies (*81*, *82*). Understanding how and whether these rare adverse events result from maladaptive immune responses induced by vaccine-vectored antigens, or whether they instead result from immune responses triggered by elements of the LNP-mRNA vaccine delivery platform is a question of key importance given the enormous clinical potential for this effective vaccine modality. Furthermore, knowledge about longitudinal clinical outcomes of SARS-CoV-2 mRNA vaccine–associated myopericarditis is currently sparse. In this study, we performed multimodal analyses in a cohort of patients who developed myocarditis and/or pericarditis after receiving an mRNA vaccine to SARS-CoV-2, comprising the first system-level analysis of the immune landscape in such patients.

In line with prior reports (*5*, *7*, *9*, *10*, *12*, *13*), the majority of patients in our cohort were adolescent or young adult males presenting a few days after the second dose of an mRNA vaccine and characterized by acute systemic inflammation, elevated troponin and BNP levels, and cardiac imaging abnormalities. First, we show that these patients did not exhibit eosinophilia or elevated T_H2 cytokines, consistent with previous observations (*7*, *9*), making alternative hypotheses of hypersensitivity or eosinophilic myocarditis (*11*, *33*) unlikely explanations of the underlying pathogenesis. In addition, our analyses of the humoral response to vaccination revealed that patients with myopericarditis generated typical or even lower SARS-CoV-2–specific antibodies and neutralizing antibody responses relative to healthy VCs, consistent with previous results (*40*). These patients also did not show evidence of cardiac-targeted autoantibodies, which have been reported in SARS-CoV-2 infection (*83*–*85*), in agreement with observations reported from one patient (*32*). Although anti–IL-1RA antibodies have been reported in some patients from another report (*80*), analysis of non-cardiac antigens in a subset of patients from our cohort showed no such autoantibodies (*86*). Consistently, our BCR repertoire analysis showed little evidence for B cell clonal expansion or somatic hypermutation in patients. These results argue that neither overexuberant nor cross-reacting humoral responses are likely explanations of the pathogenesis (*13*, *87*).

Instead, using an unbiased and system-based approach, we reveal that vaccine-associated myopericarditis patients are characterized by systemic cytokinopathy and activated cytotoxic lymphocytes with distinct transcriptional signatures consistent with their potential to mediate heart tissue damage. First, we noted an activation signature in NK cells with dysregulation of the activating receptor NKG2D, possibly linked to vaccine-associated myopericarditis. NKG2D is an activating receptor that binds stress ligands on tissues, including the heart (*88*), inducing cytotoxic effector responses (*89*–*96*). Elevation and activation of NK cells were also reported in two patients with vaccine-associated myocarditis/myopericarditis from different studies (*32*, *40*). These cellular changes were coupled with elevated serum IL-15, a potent activator of NK and T cells, among other functions (*97*–*100*). Next, we show that activated $CD4^+$ and $CD8^+$ cytotoxic T cells ($PD\text{-}1^+$ and $CD38^+$/$HLA\text{-}DR^+$) are significantly expanded in myopericarditis early after vaccination, further expressing the chemokine receptors CXCR3 and CCR5, whose ligands, CXCL10 and CCL4, respectively, were concomitantly elevated in patients′ sera. As regulators of cytotoxic T cell and T_H1 responses, these chemokines play central roles in activated T cell infiltration of cardiac tissue, as demonstrated previously across inflammatory cardiovascular diseases, including classic myocarditis (*50*–*58*). Using TCR repertoire analysis, we uncovered that these cells did not show evidence of monoclonal expansion, suggestive of an antigen-independent, cytokine-dependent activation after vaccination. T cell activation was noted in a published report from one patient presenting after the first dose of mRNA-1273 vaccination, which centered around IL-18 responses (*32*), suggesting that such a pathology likely overlaps across different clinical presentations and doses. Further, although published mechanistic studies into SARS-CoV-2 vaccine–associated myopericarditis remain scarce, reports from cardiac biopsies support our results, demonstrating lymphocytic infiltration (*34*–*36*, *80*), including $HLA\text{-}DR^+$–activated T cells (*30*). These findings are distinct from previously reported forms of vaccine-associated myocarditis (including after tetanus toxoid, conjugate meningococcal C and hepatitis B, and smallpox vaccines), where the pathologies were largely eosinophilic (*101*–*103*).

Longitudinal clinical follow-up months after vaccination revealed persistent cardiac imaging abnormalities in some patients, most notably LGE on CMR imaging, suggesting cardiac fibrosis (*104*–*106*). We additionally observed elevations in various serum extracellular matrix remodeling enzymes (MMP1, MMP8, MMP9, and TIMP1), increased inflammatory classical monocytes ($CCR2^+$ $CD163^+$) carrying a profibrotic signature, and elevation in sCD163, indicative of cardiac macrophage activation. Our clinical, cellular, and molecular findings potentially point to ongoing wound healing, tissue remodeling, and scar formation after cardiac injury in these patients (*39*, *107*–*111*). Released damage-associated signals, in addition to elevation of the proinflammatory cytokine IL-1β as seen in patients′ sera, triggered by cardiac injury can induce monocyte/macrophage recruitment, further exacerbating the inflammation in myocarditis and/or resulting in tissue fibrosis (*39*, *74*, *76*). These results are supported by published cardiac biopsy reports showing macrophage infiltration of heart tissue (*34*–*36*). Most recently, a large clinical study of 69 total patients with clinically suspected SARS-CoV-2 vaccine–associated myocarditis reported 40 biopsy-confirmed cases with prominent T cell and macrophage infiltration of cardiac tissue (*80*). In one report, overlapping immune infiltrate of T cells and macrophages was additionally found at the vaccine injection site in the deltoid muscle (*112*). Another histopathological study of 15 clinically suspected cases further reported cardiac infiltration of $HLA\text{-}DR^+$ T cells and $MAC\text{-}1^+$ macrophages (*30*), which are consistent with the aberrant immune cell subsets we define here. Thus, our molecular and cellular immunological findings here are supported by published histological evidence, presenting the first characterization of these most likely pathogenic inflammatory cell subpopulations.

The question of why such adverse events develop more frequently after the second dose is intriguing. Recent system vaccinology approaches revealed that the BNT162b2 mRNA vaccine stimulated only modest innate immune responses after the first dose. These responses were substantially enhanced after secondary immunization (*59*). The authors further reported a significant increase in plasma IFN-γ and CXCL10 (also known as IFN-γ–induced protein 10) shortly after secondary immunization, proposing a "cytokine feedback" model that regulates innate immune responses. In addition, effective mRNA vaccine responses have also been described to induce systemic IL-15 (*113*), and other cytokines may be acting locally in the tissue (i.e., not measurably increased in systemic circulation) to potentially drive cytotoxic lymphocyte responses in myopericarditis. IFN-γ further correlated with pSTAT3 levels, which peaked 1 day after secondary vaccination in HDs across several cell types (*59*). In patients with myopericarditis here, pSTAT3 levels in $CD8^+$ T cells were elevated several days after vaccination during hospitalization, consistent with sustained cytokinopathy after vaccination. IFN-γ is known to enhance HLA-DR expression on T cells during activation, as observed in our patients, which is further seen in CTL heart infiltration in myocarditis (*114*). In addition, CXCR3, the activated T cell homing receptor for IFN-γ–induced CXCL10, has been characterized to facilitate the differentiation of $CD8^+$ T cells into short-lived effector, rather than long-lived memory, cells by mediating cell migration based on the strength of the inflammatory stimulus (*115*–*117*), which may suggest reduced long-term T cell memory responses to vaccination in such patients, with important implications for effective vaccine development. These accumulating pieces of evidence complement our observations, whereby susceptible individuals may experience a heightened cytokine-driven immune response to vaccination and, particularly, shortly after the second dose, consequently activating immune effectors and provoking heart inflammation. Whether such responses are governed by virtual memory responses (*118*) or epigenetic reprogramming of effector subsets and/or innate immune memory (*119*–*122*) is a fundamental question warranting future investigation.

Although the LNP component of the vaccine alone was found to be highly inflammatory, such responses centered on IL-6 and IL-1β (*41*, *123*). IL-1β was elevated in our cohort of patients and together with upstream NLRP3 inflammasome activation and associated cytokines may play a role in the pathogenesis of myocarditis (*32*, *39*). However, IL-1β induction by lipid-formulated RNA vaccines, which can then stimulate various proinflammatory cytokines, was also shown to be dependent on both the RNA and lipid formulation in human immune cells (*124*). Thus, a compound role of the adjuvant delivery platform in synergy with vaccine-vectored antigens is more likely the driver of an exaggerated immune cytokine response driving cardiac pathology after vaccination in susceptible individuals. What causes certain individuals, notably adolescent and young adult males, to be more susceptible to these cardiac-related adverse events is not clear but likely not unique to vaccine-induced pathogenesis. A bias toward younger males is similarly seen in community-acquired myocarditis/pericarditis, where many large-scale epidemiological and clinical studies have demonstrated that patients are much more frequently males (65 to 84% of patients) and significantly younger than female patients (*125*–*136*), potentially suggesting heightened immune and/or inflammatory responses in these demographic groups.

Our study has some limitations. Although our cohort of LNP-mRNA vaccine-associated myopericarditis is one of the largest studied to date, and our hypothesis is consistent with published reports from other patients, the number of participants remains limited to make broad conclusions. In addition, despite using several control groups to ensure that our findings are unique to vaccine-associated myopericarditis, variations in age, vaccine dose, or time after vaccination across individuals are considerations for interpretation and broad conclusions. Our high-throughput autoantibody analysis by REAP also focused on extracellular/secreted antigens, so intracellular autoantigens may still play a role in the pathogenesis, although this was not supported in previous studies (*32*). In addition, the contribution of genetic variants that may influence myocarditis susceptibility has not yet been determined and is an active area of investigation. Last, our study did not have tissue samples to confirm the effector immune population infiltrating the heart, yet our results agree with previously published biopsy reports.

On the basis of our findings, longitudinal clinical monitoring of vaccine-associated myopericarditis patients may be warranted to assess potential persistence of cardiac abnormalities. It is also critical to contextualize the rare risk of adverse events and potential clinical sequelae after SARS-CoV-2 vaccination (*2*, *5*) in comparison with the greater risks of sequelae (including myocarditis), hospitalization, and/or death resulting from infection with SARS-CoV-2 (*5*, *24*, *137*–*140*). Our study leverages a rare patient cohort and presents findings with potential implications for vaccine development and clinical care. Future studies building on the translational relevance of our work will be important to further optimize the excellent safety profile of mRNA vaccines among specific demographic subgroups. In conclusion, our findings likely rule out some previously proposed mechanisms of mRNA vaccine–associated myopericarditis and implicate aberrant cytokine-driven lymphocyte activation and cytotoxicity as well as inflammatory and profibrotic myeloid cell responses in the immunopathology occurring in susceptible patients after mRNA vaccination.

MATERIALS AND METHODS

Study design

The primary aim of this study was to investigate the systemic immunopathological landscape underlying rare cases of myopericarditis occurring after SARS-CoV-2 LNP-mRNA vaccination. A total cohort of 23 patients developing myocarditis and/or pericarditis with elevated troponin, BNP, and CRP levels as well as cardiac imaging abnormalities shortly after vaccination was compared with healthy VCs, among other groups. Different subsets of these patients were profiled using multimodal approaches, including SARS-CoV-2 antibodies and neutralization, high-throughput exoproteome cardiac autoantibody profiling, serum proteomics, flow cytometry, ELISA, and peripheral blood single-cell transcriptome and repertoire sequencing to define immunopathological alterations. Last, clinical follow-up including CMR imaging was conducted between 2 to 9 months after vaccination to assess potential long-term disease effects.

Human participant research

Human participants in this study provided informed consent to use their samples for research and to publish de-identified data in accordance with Helsinki principles for enrollment in research

protocols that were approved by the Institutional Review Board (IRB) of Yale University (protocols 2000028924 and 1605017838). For a subset of patients, whose inclusion was solely for medical record review for population surveillance and vaccine investigations, the IRB approved the study and waived the requirement for informed consent (protocol 2000028093). All relevant ethical regulations for work with human participants were followed.

Blood sample processing

For the antibody, neutralization, REAP, and cytokine assays, whole blood was collected in heparinized CPT blood vacutainers (BDAM362780, BD) and processed on the same day of collection. Plasma samples were collected after centrifugation of whole blood at 600*g* for 20 min at room temperature. Undiluted plasma was transferred to 1.8-ml Eppendorf polypropylene tubes and stored at −80°C for subsequent analysis. For blood clinical parameters, significance was determined through comparison against normal reference ranges used at Yale New Haven Hospital for each test.

For the scRNA-seq analysis, PBMCs were first isolated by Ficoll-Paque Plus (GE Healthcare) or Lymphoprep (STEMCELL Technologies) density gradient centrifugation. Cells were subsequently washed twice in phosphate-buffered saline (PBS) and resuspended in complete RPMI 1640 (cRPMI) medium (Lonza) containing 10% fetal bovine serum (FBS), 2 mM glutamine, and penicillin and streptomycin (100 U/ml each; Invitrogen). PBMCs were then stored at 10^6 cells per ml in 10% dimethyl sulfoxide in FBS and stored in −80°C overnight before further storage in liquid nitrogen. Serum was isolated by centrifugation of serum tubes and saving the supernatant in aliquots, which were flash-frozen in liquid nitrogen before cryopreservation in −80°C. All patient PBMCs were processed and cryopreserved within 1 to 6 hours of blood draw. HD PBMCs were all processed within 24 hours to account for overnight shipping.

SARS-CoV-2–specific antibodies

ELISA was performed as previously described (*141*). In short, Triton X-100 and ribonuclease A were added to serum samples at final concentrations of 0.5% and 0.5 mg/ml, respectively, and incubated at room temperature for 30 min before use to reduce risk from any potential virus in serum. MaxiSorp plates (96 wells; 442404, Thermo Fisher Scientific) were coated with recombinant SARS-CoV-2 S total (50 μl per well; 100 μg; SPN-C52H9, ACROBiosystems), S1 (100 μg; S1N-C52H3, ACROBiosystems), and RBD (100 μg; SPD-C52H3, ACROBiosystems) at a concentration of 2 μg/ml in PBS and were incubated overnight at 4°C. The coating buffer was removed, and plates were incubated for 1 hour at room temperature with 200 μl of blocking solution [PBS with 0.1% Tween 20 (PBS-T) and 3% milk powder]. Plasma was diluted serially at 1:100, 1:200, 1:400, and 1:800 in dilution solution (PBS-T and 1% milk powder), and 100 μl of diluted serum were added for 2 hours at room temperature. Human anti-spike (SARS-CoV-2 human anti-spike clone AM006415; 91351, Active Motif) and anti-nucleocapsid (SARS-CoV-2 human anti-nucleocapsid clone 1A6; MA5-35941, Invitrogen) were serially diluted to generate a standard curve. Plates were washed three times with PBS-T, and 50 μl of horseradish peroxidase anti-human IgG antibody (1:5000; A00166, GenScript) diluted in dilution solution were added to each well. After 1 hour of incubation at room temperature, plates were washed six times with PBS-T. Plates were developed with 100 μl of 3,3′,5,5′-tetramethylbenzidine (TMB) substrate reagent set (555214, BD Biosciences), and the reaction was stopped after 5 min by the addition of 2 N sulfuric acid. Plates were then read at wavelengths of 450 nm and 570 nm.

Cell lines and virus

Vero E6 kidney epithelial cells (C1008, CRL-1586) were cultured in Dulbecco's modified Eagle's medium (DMEM) supplemented with 1% sodium pyruvate, nonessential amino acids, and 5% FBS at 37°C and 5% CO_2. The cell line was obtained from the American Type Culture Collection and was negative for contamination with *Mycoplasma* using commercially available kits. SARS-CoV-2 (ancestral strain, D614G) USA-WA1/2020 was obtained from BEI Resources (NR-52281) and minimally amplified in Vero E6 cells to generate working stocks of virus. All experiments were performed in a Biosafety Level 3 facility with approval from the Yale Environmental Health and Safety office.

Neutralization assay

Patient and VC sera were isolated as above and heat-treated for 30 min at 56°C. Plasma was serially diluted from 1:10 to 1:2430 and incubated with SARS-CoV-2 (ancestral strain, D614G) for 1 hour at 37°C. Inoculum was subsequently incubated with Vero E6 cells in a six-well plate for 1 hour for adsorption. Next, infected cells were overlayed with DMEM supplemented with $NaHCO_3$, 2% FBS, and 0.6% Avicel mixture. Plaques were resolved at 40 hours after infection by fixing in 4% formaldehyde for 1 hour followed by staining in 0.5% crystal violet. All experiments were performed in parallel with negative control sera with an established viral concentration sufficient to generate 60 to 120 plaques in control wells.

REAP

Antibody purification, yeast adsorption and library selections, NGS library preparation, and REAP score calculation were performed as previously described (*43*, *44*, *86*). A more detailed protocol is also included in Supplementary Methods.

Cytokine analysis

Plasma was isolated from patients as described above. Levels of cytokines were assessed using commercially available vendors, described at length previously (*142*). Briefly, sera were shipped to Eve Technologies (Calgary, Alberta, Canada) on dry ice, and levels of cytokines and chemokines were measured using the Human Cytokine Array/Chemokine Array 71-403 Plex Panel (HD71) and the Human Matrix Metalloprotease Panel (HDMYO-3-12). All samples were measured upon first thaw. Samples below the range of detection were replaced with the lowest observed value for quantitation.

PCA and hierarchical clustering were performed using MATLAB 2020b (MathWorks Inc.) using standard built-in functions. Gene enrichment was performed on identified clusters using GO analysis to identify significance, and the top 10 hierarchical, biological processes were reported (*143*, *144*).

ELISA

Serum was isolated as above alongside PBMC isolation, flash-frozen, and stored at −80°C until further use. Serum was then thawed at 37°C and plated in duplicate or triplicate. Standards were made fresh for each assay. The assays were run using the ELISA MAX Deluxe Set Human IL-15 (BioLegend, catalog no.

435104) and the CD163 Human ELISA (Thermo Fisher Scientific, catalog no. EHCD163) kits following the manufacturer's instructions.

scRNA-seq and alignment

Cryopreserved PBMCs were thawed in a water bath at 37°C for ~2 min and removed from the water bath when a tiny ice crystal remained. Cells were transferred to a 15-ml conical tube of prewarmed growth medium. The cryovial was rinsed with additional growth medium (10% FBS in DMEM) to recover leftover cells, and the rinse medium was added to the 15-ml conical tube while gently shaking the tube.

Thawed PBMCs were centrifuged at 400*g* for 8 min at room temperature, and the supernatant was removed without disrupting the cell pellet. The pellet was resuspended in 1× PBS with 2% FBS, and cells were filtered with a 30-μM cell strainer. The cellular concentration was adjusted to 1000 cells per μl on the basis of the cell count, and cells were immediately loaded onto the 10x Chromium Next GEM Chip G according to the manufacturer's user guide [Chromium Next GEM SingleCell V(D)J Reagent Kits v1.1]. We aimed to obtain a yield of ~10,000 cells per lane.

cDNA libraries for gene expression and TCR/BCR sequencing were generated according to the manufacturer's instructions (Chromium Next GEM SingleCell V(D)J Reagent Kits v1.1). Each library was then sequenced on an Illumina NovaSeq 6000 platform. The single-cell transcriptome sequencing data were processed using CellRanger v5.0.1 and aligned to the GRCh38 reference genome (*145*). CITE-seq surface protein reads were quantified using a provided tagged antibodies dictionary.

Quality control, preprocessing, and integration

After data alignment and quantification, we performed quality control assessment before proceeding with data processing and downstream analysis. First, genes expressed in fewer than five cells and cells with fewer than 200 genes or more than 10% mitochondrial gene fraction were removed.

The filtered single-cell data were thereafter integrated, and batch effects were corrected using single-cell variational inference (scVI) (*146*) with a generative model of 64 latent variables and 500 iterations. More specifically, scVI's negative binomial model was used on raw counts, selecting 5000 highly variable genes identified by the tool's native method in the combined datasets to produce latent variables. To minimize the dependence of clustering on cell cycle effects, previously defined cell cycle phase–specific genes in the Seurat package (*147*) were excluded from this list of highly variable genes. Data from patients with acute myopericarditis, E-YVCs, recovered patients, and HDs were integrated for downstream analysis. Four MIS-C CITE-seq samples were also included to aid with cell annotation using surface protein markers.

The latent representation generated by scVI was used to compute the neighborhood graph (*scanpy.pp.neighbors*), which was used for Louvain clustering (*scanpy.tl.louvain*) and Uniform Manifold Approximation and Projection (UMAP) visualization (*scanpy.tl.umap*).

Before clustering, to aid with cell annotation, Single-Cell Remover of Doublets (Scrublet) (*148*) was used to preliminary label doublets by computing a doublet score for each cell. In particular, a Student's *t* test ($P < 0.01$) and Bonferroni correction were used within fine-grained subclustering of each cluster initially identified by the Louvain algorithm.

Data processing was performed using the Scanpy toolkit (*149*) following published recommended standard practices. Before downstream analysis, data were normalized (*scanpy.pp.normalize_per_cell*, scaling factor = 10^4) and log-transformed (*scanpy.pp.log1p*). For heatmaps of gene expression, the data were further scaled (*scanpy.pp.scale*, max value = 10).

Cluster identification and immune subset annotation

First, a logistic regression model was used to transfer preliminary cell annotations from our previous published MIS-C dataset (*63*) using highly variable genes (*scanpy.pp.highly_variable_genes*) shared between the two datasets to guide cluster identification. Thereafter, clustering was performed using the Louvain algorithm with an initial resolution of three, and the resulting clusters were defined on the basis of the expression of published cell-specific gene markers. For ambiguous clusters, differential gene expression analysis compared with all other clusters was performed (*scanpy.tl.rank_genes_groups*), and the resulting top genes were used for unbiased determination of cell identity.

The initial doublet predications by Scrublet were revised here, and doublets were confirmed on the basis of cluster coexpression of heterogeneous lineage gene markers (e.g., *CD3*, *CD19*, and *CD14*) along with the n_counts and n_genes distributions. In addition to removing doublets, clusters displaying patterns of dying cells with high mitochondrial content were further removed. Refined subclusters were used for downstream data analysis and visualization, including cell type frequency, differential gene expression, and repertoire analyses.

Cell subset proportions

To determine significant changes in the proportions of identified subsets across the groups while accounting for compositional dependencies between the subsets in the scRNA-seq data, we used the Bayesian model scCODA (*49*). Specifically, for each subset, the myopericarditis group was compared with the E-YVC group, and default parameters were used. Changes classified by scCODA as credible after correction for multiple comparisons (FDR < 0.05) were considered statistically significant. In some cases where changes were not classified as significant by scCODA's method, we used the nonparametric unpaired two-sided Wilcoxon rank-sum test with Benjamini-Hochberg FDR correction for multiple comparisons as previously described (*150*), and we report the exact adjusted *P* value, given that such changes may still be biologically meaningful.

Differential gene expression

The limma package (*151*) was used to obtain differentially expressed genes (FDR < 0.05). The analysis was performed either comparing different cell subsets or in the same cell subset comparing cells from different groups. Top differentially expressed genes by logFC (up-regulated and down-regulated) and published pathway gene sets were used for plotting and heatmap visualization after data scaling.

Gene expression scores

Published gene sets from the MSigDB were used to calculate the average enrichment scores across cells of defined subsets as

specified in the figure legends using the *scanpy.tl.score_genes* function with default parameters.

Mapping annotations between datasets

For mapping single-cell immune populations between datasets, a logistic regression model was used using scikit-learn with default parameters. For heart cells, T lymphocyte subsets from published single-cell data (*60*) were used to train the model using expression data of highly variable genes (*scanpy.pp.highly_variable_genes*) shared between the two datasets. The model was then applied to predict matching cell subsets in our dataset (mean prediction probability = 0.9), and the percentage of cells mapping between subsets was visualized.

TCR repertoire analysis

TCR diversity, gene usage, and clonotype analyses were done as previously described (*63*). A more detailed protocol is also included in Supplementary Methods.

BCR repertoire analysis

Analysis of the BCR repertoire was performed as previously described (*63*) using the Immcantation framework as listed above in the TCR analysis, and annotations were incorporated from overall PBMC clustering for B cell subsets.

Flow cytometry

Patient and donor PBMCs were thawed as above and rested in cRPMI for 2 hours at 37°C before staining. The cells were counted, resuspended in PBS, and stained with e780 Fixable Viability Dye (eBioscience, catalog no. 65-0865-14) for 15 min on ice. The cells were then washed and resuspended in PBS with 10% FBS, with Human TruStain FcX (BioLegend, catalog no. 422302) and True-Stain Monocyte Blocker (BioLegend, catalog no. 426102) for 15 min on ice. The cells were then stained with surface antibody cocktails for 25 min on ice. For phospho-staining, cells were first treated with Fc blocker and then fixed and permeabilized with methanol before staining for intracellular proteins. All flow cytometry data were acquired on the LSR Fortessa cytometer, and gating strategies are shown in figs. S9 and S10. Further details about flow cytometry antibodies are included in Supplementary Methods.

Statistical analysis

Data were analyzed by various statistical tests as described in detail in the corresponding individual figure captions. For all comparisons, error bars, exact *P* values, and testing levels were shown whenever possible, and corrections for multiple comparisons were done when appropriate.

Supplementary Materials

This PDF file includes:
Supplementary Methods
Tables S1 and S2
Figs. S1 to S10
References (*152*–*154*)

Other Supplementary Material for this manuscript includes the following:
Table S3
Data file S1
MDAR Reproducibility Checklist

View/request a protocol for this paper from *Bio-protocol*.

REFERENCES AND NOTES

1. L. R. Baden, H. M. El Sahly, B. Essink, K. Kotloff, S. Frey, R. Novak, D. Diemert, S. A. Spector, N. Rouphael, C. B. Creech, J. M. Gettigan, S. Khetan, N. Segall, J. Solis, A. Brosz, C. Fierro, H. Schwartz, K. Neuzil, L. Corey, P. Gilbert, H. Janes, D. Follmann, M. Marovich, J. Mascola, L. Polakowski, J. Ledgerwood, B. S. Graham, H. Bennett, R. Pajon, C. Knightly, B. Leav, W. Deng, H. Zhou, S. Han, M. Ivarsson, J. Miller, T. Zaks; COVE Study Group, Efficacy and safety of the mRNA-1273 SARS-CoV-2 Vaccine. *N. Engl. J. Med.* **384**, 403–416 (2021).
2. N. Barda, N. Dagan, Y. Ben-Shlomo, E. Kepten, J. Waxman, R. Ohana, M. A. Hernán, M. Lipsitch, I. Kohane, D. Netzer, B. Y. Reis, R. D. Balicer, Safety of the BNT162b2 mRNA Covid-19 vaccine in a nationwide setting. *N. Engl. J. Med.* **385**, 1078–1090 (2021).
3. F. P. Polack, S. J. Thomas, N. Kitchin, J. Absalon, A. Gurtman, S. Lockhart, J. L. Perez, G. Pérez Marc, E. D. Moreira, C. Zerbini, R. Bailey, K. A. Swanson, S. Roychoudhury, K. Koury, P. Li, W. V. Kalina, D. Cooper, R. W. Frenck Jr., L. L. Hammitt, Ö. Türeci, H. Nell, A. Schaefer, S. Ünal, K. U. Jansen, W. C. Gruber; C4591001 Clinical Trial Group, Safety and efficacy of the BNT162b2 mRNA covid-19 vaccine. *N. Engl. J. Med.* **383**, 2603–2615 (2020).
4. T. T. Shimabukuro, S. Y. Kim, T. R. Myers, P. L. Moro, T. Oduyebo, L. Panagiotakopoulos, P. L. Marquez, C. K. Olson, R. Liu, K. T. Chang, S. R. Ellington, V. K. Burkel, A. N. Smoots, C. J. Green, C. Licata, B. C. Zhang, M. Alimchandani, A. Mba-Jonas, S. W. Martin, J. M. Gee, D. M. Meaney-Delman; CDC v-safe COVID-19 Pregnancy Registry Team, Preliminary findings of mRNA covid-19 vaccine safety in pregnant persons. *N. Engl. J. Med.* **384**, 2273–2282 (2021).
5. M. Patone, X. W. Mei, L. Handunnetthi, S. Dixon, F. Zaccardi, M. Shankar-Hari, P. Watkinson, K. Khunti, A. Harnden, C. A. C. Coupland, K. M. Channon, N. L. Mills, A. Sheikh, J. Hippisley-Cox, Risks of myocarditis, pericarditis, and cardiac arrhythmias associated with COVID-19 vaccination or SARS-CoV-2 infection. *Nat. Med.* **28**, 410–422 (2021).
6. H. G. Rosenblum, J. Gee, R. Liu, P. L. Marquez, B. Zhang, P. Strid, W. E. Abara, M. M. McNeil, T. R. Myers, A. M. Hause, J. R. Su, L. E. Markowitz, T. T. Shimabukuro, D. K. Shay, Safety of mRNA vaccines administered during the initial 6 months of the US COVID-19 vaccination programme: An observational study of reports to the vaccine adverse event reporting system and v-safe. *Lancet Infect. Dis.* **22**, 802–812 (2022).
7. B. Bozkurt, I. Kamat, P. J. Hotez, Myocarditis with COVID-19 mRNA vaccines. *Circulation* **144**, 471–484 (2021).
8. G. A. Diaz, G. T. Parsons, S. K. Gering, A. R. Meier, I. V. Hutchinson, A. Robicsek, Myocarditis and pericarditis after vaccination for COVID-19. *JAMA* **326**, 1210–1212 (2021).
9. K. F. Larson, E. Ammirati, E. D. Adler, L. T. Cooper Jr., K. N. Hong, G. Saponara, D. Couri, A. Cereda, A. Procopio, C. Cavalotti, F. Oliva, T. Sanna, V. A. Ciconte, G. Onyango, D. R. Holmes, D. D. Borgeson, Myocarditis after BNT162b2 and mRNA-1273 vaccination. *Circulation* **144**, 506–508 (2021).
10. M. Marshall, I. D. Ferguson, P. Lewis, P. Jaggi, C. Gagliardo, J. S. Collins, R. Shaughnessy, R. Caron, C. Fuss, K. J. E. Corbin, L. Emuren, E. Faherty, E. K. Hall, C. di Pentima, M. E. Oster, E. Paintsil, S. Siddiqui, D. M. Timchak, J. A. Guzman-Cottrill, Symptomatic acute myocarditis in 7 adolescents after Pfizer-BioNTech COVID-19 vaccination. *Pediatrics* **148**, e2021052478 (2021).
11. J. Montgomery, M. Ryan, R. Engler, D. Hoffman, B. McClenathan, L. Collins, D. Loran, D. Hrncir, K. Herring, M. Platzer, N. Adams, A. Sanou, L. T. Cooper Jr., Myocarditis following immunization with mRNA COVID-19 vaccines in members of the US military. *JAMA Cardiol.* **6**, 1202–1206 (2021).
12. C. M. Rosner, L. Genovese, B. N. Tehrani, M. Atkins, H. Bakhshi, S. Chaudhri, A. A. Damluji, J. A. de Lemos, S. S. Desai, A. Emaminia, M. C. Flanagan, A. Khera, A. Maghsoudi, G. Mekonnen, A. Muthukumar, I. M. Saeed, M. W. Sherwood, S. S. Sinha, C. M. O'Connor, C. R. deFilippi, Myocarditis temporally associated with COVID-19 vaccination. *Circulation* **144**, 502–505 (2021).
13. S. Heymans, L. T. Cooper, Myocarditis after COVID-19 mRNA vaccination: Clinical observations and potential mechanisms. *Nat. Rev. Cardiol.* **19**, 75–77 (2022).
14. S. Le Vu, M. Bertrand, M.-J. Jabagi, J. Botton, J. Drouin, B. Baricault, A. Weill, R. Dray-Spira, M. Zureik, Age and sex-specific risks of myocarditis and pericarditis following Covid-19 messenger RNA vaccines. *Nat. Commun.* **13**, 3633 (2022).
15. F.B. Document, Vaccines and Related Biological Products Advisory Committee Meeting (U.S. Food and Drug Administration, 2022).
16. K. Goddard, K. E. Hanson, N. Lewis, E. Weintraub, B. Fireman, N. P. Klein, Incidence of myocarditis/pericarditis following mRNA COVID-19 vaccination among children and younger adults in the United States. *Ann. Intern. Med.* **175**, 1169–1771 (2022).
17. A. B. Hause, J. Baggs, P. Marquez, W. E. Abara, B. Olubajo, T. R. Myers, J. R. Su, D. Thompson, J. Gee, T. T. Shimabukuro, D. K. Shay, Safety monitoring of COVID-19 vaccine booster

doses among persons aged 12–17 years — United States, December 9, 2021–February 20, 2022. *MMWR Morb. Mortal. Wkly Rep.* **71**, 347–351 (2022).
18. S. Lane, A. Yeomans, S. Shakir, Reports of myocarditis and pericarditis following mRNA COVID-19 vaccination: A systematic review of spontaneously reported data from the UK, Europe and the USA and of the scientific literature. *BMJ Open* **12**, e059223 (2022).
19. B. Mengesha, A. G. Asenov, B. Hirsh-Raccah, O. Amir, O. Pappo, R. Asleh, Severe acute myocarditis after the third (booster) dose of mRNA COVID-19 vaccination. *Vaccines* **10**, 575 (2022).
20. W. F. Gellad, Myocarditis after vaccination against covid-19. *BMJ* **375**, n3090 (2021).
21. A. Husby, J. V. Hansen, E. Fosbøl, E. M. Thiesson, M. Madsen, R. W. Thomsen, H. T. Sørensen, M. Andersen, J. Wohlfahrt, G. Gislason, C. Torp-Pedersen, L. Køber, A. Hviid, SARS-CoV-2 vaccination and myocarditis or myopericarditis: Population based cohort study. *BMJ* **375**, e068665 (2021).
22. M. E. Oster, D. K. Shay, J. R. Su, J. Gee, C. B. Creech, K. R. Broder, K. Edwards, J. H. Soslow, J. M. Dendy, E. Schlaudecker, S. M. Lang, E. D. Barnett, F. L. Ruberg, M. J. Smith, M. J. Campbell, R. D. Lopes, L. S. Sperling, J. A. Baumblatt, D. L. Thompson, P. L. Marquez, P. Strid, J. Woo, R. Pugsley, S. Reagan-Steiner, F. De Stefano, T. T. Shimabukuro, Myocarditis cases reported after mRNA-based COVID-19 vaccination in the US from December 2020 to August 2021. *JAMA* **327**, 331–340 (2022).
23. G. Witberg, N. Barda, S. Hoss, I. Richter, M. Wiessman, Y. Aviv, T. Grinberg, O. Auster, N. Dagan, R. D. Balicer, R. Kornowski, Myocarditis after Covid-19 vaccination in a large health care organization. *N. Engl. J. Med.* **385**, 2132–2139 (2021).
24. J. P. Block, T. K. Boehmer, C. B. Forrest, T. W. Carton, G. M. Lee, U. A. Ajani, D. A. Christakis, L. G. Cowell, C. Draper, N. Ghildayal, A. M. Harris, M. D. Kappelman, J. Y. Ko, K. H. Mayer, K. Nagavedu, M. E. Oster, A. Paranjape, J. Puro, M. D. Ritchey, D. K. Shay, D. Thacker, A. V. Gundlapalli, Cardiac complications after SARS-CoV-2 infection and mRNA COVID-19 vaccination—PCORnet, United States, January 2021–January 2022. *MMWR Morb Mortal Wkly Rep.* **71**, 517–523 (2022).
25. A. Fleming-Nouri, A. D. Haimovich, D. Yang, W. L. Schulz, A. Coppi, R. A. Taylor, Myopericarditis in young adults presenting to the emergency department after receiving a second COVID-19 mRNA vaccine. *Acad. Emerg. Med.* **28**, 802–805 (2021).
26. *Dose-Finding Trial to Evaluate the Safety and Immunogenicity of Cytomegalovirus (CMV) Vaccine mRNA-1647 in Healthy Adults* (Clinicaltrials.gov., NCT04232280); https://clinicaltrials.gov/ct2/show/NCT04232280.
27. *Trial With BNT111 and Cemiplimab in Combination or as Single Agents in Patients With Anti-PD1-refractory/Relapsed, Unresectable Stage III or IV Melanoma* (Clinicaltrials.gov., NCT04526899); https://clinicaltrials.gov/ct2/show/NCT04526899.
28. *An Efficacy Study of Adjuvant Treatment With the Personalized Cancer Vaccine mRNA-4157 and Pembrolizumab in Participants With High-Risk Melanoma (KEYNOTE-942)* (NCI, NCT03897881); www.cancer.gov/about-cancer/treatment/clinical-trials/search/v?id=NCI-2019-04957&r=1.
29. L. M. Yonker, Z. Swank, Y. C. Bartsch, M. D. Burns, A. Kane, B. P. Boribong, J. P. Davis, M. Loiselle, T. Novak, Y. Senussi, C. A. Cheng, E. Burgess, A. G. Edlow, J. Chou, A. Dionne, D. Balaguru, M. Lahoud-Rahme, M. Arditi, B. Julg, A. G. Randolph, G. Alter, A. Fasano, D. R. Walt, Circulating spike protein detected in post-COVID-19 mRNA vaccine myocarditis. *Circulation* **147**, 867–876 (2023).
30. C. Baumeier, G. Aleshcheva, D. Harms, U. Gross, C. Hamm, B. Assmus, R. Westenfeld, M. Kelm, S. Rammos, P. Wenzel, T. Münzel, A. Elsässer, M. Gailani, C. Perings, A. Bourakkadi, M. Flesch, T. Kempf, J. Bauersachs, F. Escher, H. P. Schultheiss, Intramyocardial inflammation after COVID-19 vaccination: An endomyocardial biopsy-proven case series. *Int. J. Mol. Sci.* **23**, 6940 (2022).
31. D. Marrama, J. Mahita, A. Sette, B. Peters, Lack of evidence of significant homology of SARS-CoV-2 spike sequences to myocarditis-associated antigens. *EBioMedicine* **75**, 103807 (2022).
32. T. Won, N. A. Gilotra, M. K. Wood, D. M. Hughes, M. V. Talor, J. Lovell, A. M. Milstone, C. Steenbergen, D. Čiháková, Increased interleukin 18-dependent immune responses are associated with myopericarditis after COVID-19 mRNA vaccination. *Front. Immunol.* **13**, 851620 (2022).
33. T. D'Angelo, A. Cattafi, M. L. Carerj, C. Booz, G. Ascenti, G. Cicero, A. Blandino, S. Mazziotti, Myocarditis after SARS-CoV-2 vaccination: A vaccine-induced reaction? *Can. J. Cardiol.* **37**, 1665–1667 (2021).
34. P. Ehrlich, K. Klingel, S. Ohlmann-Knafo, S. Hüttinger, N. Sood, D. Pickuth, M. Kindermann, Biopsy-proven lymphocytic myocarditis following first mRNA COVID-19 vaccination in a 40-year-old male: Case report. *Clin. Res. Cardiol.* **110**, 1855–1859 (2021).
35. S. Kazama, T. Okumura, Y. Kimura, R. Ito, T. Araki, T. Mizutani, H. Oishi, T. Kuwayama, H. Hiraiwa, T. Kondo, R. Morimoto, T. Saeki, T. Murohara, Biopsy-proven fulminant myocarditis requiring mechanical circulatory support following COVID-19 mRNA vaccination. *CJC Open* **4**, 501–505 (2022).
36. D. Kiblboeck, K. Klingel, M. Genger, S. Traxler, N. Braunsteiner, C. Steinwender, J. Kellermair, Myocarditis following mRNA COVID-19 vaccination: Call for endomyocardial biopsy. *ESC Heart Fail* **9**, 1996–2002 (2022).
37. A. K. Verma, K. J. Lavine, C. Y. Lin, Myocarditis after Covid-19 mRNA vaccination. *N. Engl. J. Med.* **385**, 1332–1334 (2021).
38. J. M. Myers, L. T. Cooper, D. C. Kem, S. Stavrakis, S. D. Kosanke, E. M. Shevach, D. L. Fairweather, J. A. Stoner, C. J. Cox, M. W. Cunningham, Cardiac myosin-Th17 responses promote heart failure in human myocarditis. *JCI Insight* **1**, e85851 (2016).
39. C. Tschöpe, E. Ammirati, B. Bozkurt, A. L. P. Caforio, L. T. Cooper, S. B. Felix, J. M. Hare, B. Heidecker, S. Heymans, N. Hübner, S. Kelle, K. Klingel, H. Maatz, A. S. Parwani, F. Spillmann, R. C. Starling, H. Tsutsui, P. Seferovic, S. van Linthout, Myocarditis and inflammatory cardiomyopathy: Current evidence and future directions. *Nat. Rev. Cardiol.* **18**, 169–193 (2021).
40. A. Muthukumar, M. Narasimhan, Q. Z. Li, L. Mahimainathan, I. Hitto, F. Fuda, K. Batra, X. Jiang, C. Zhu, J. Schoggins, J. B. Cutrell, C. L. Croft, A. Khera, M. H. Drazner, J. L. Grodin, B. M. Greenberg, P. P. A. Mammen, S. J. Morrison, J. A. de Lemos, In-depth evaluation of a case of presumed myocarditis after the second dose of COVID-19 mRNA vaccine. *Circulation* **144**, 487–498 (2021).
41. S. Ndeupen, Z. Qin, S. Jacobsen, A. Bouteau, H. Estanbouli, B. Z. Igyártó, The mRNA-LNP platform's lipid nanoparticle component used in preclinical vaccine studies is highly inflammatory. *iScience* **24**, 103479 (2021).
42. D. Tsilingiris, N. G. Vallianou, I. Karampela, J. Liu, M. Dalamaga, Potential implications of lipid nanoparticles in the pathogenesis of myocarditis associated with the use of mRNA vaccines against SARS-CoV-2. *Metabol. Open* **13**, 100159 (2022).
43. E. Y. Wang, Y. Dai, C. E. Rosen, M. M. Schmitt, M. X. Dong, E. M. N. Ferré, F. Liu, Y. Yang, J. A. González-Hernández, E. Meffre, M. Hinchcliff, F. Koumpouras, M. S. Lionakis, A. M. Ring, High-throughput identification of autoantibodies that target the human exoproteome. *Cell Rep. Methods* **2**, 100172 (2022).
44. E. Y. Wang, T. Mao, J. Klein, Y. Dai, J. D. Huck, J. R. Jaycox, F. Liu, T. Zhou, B. Israelow, P. Wong, A. Coppi, C. Lucas, J. Silva, J. E. Oh, E. Song, E. S. Perotti, N. S. Zheng, S. Fischer, M. Campbell, J. B. Fournier, A. L. Wyllie, C. B. F. Vogels, I. M. Ott, C. C. Kalinich, M. E. Petrone, A. E. Watkins; Yale IMPACT Team, A. Obaid, A. J. Moore, A. Casanovas-Massana, A. Lu-Culligan, A. Nelson, A. Nunez, A. Martin, B. Geng, C. D. Odio, C. A. Harden, C. Todeasa, C. Jensen, D. Kim, D. McDonald, D. Shepard, E. Courchaine, E. B. White, E. Silva, E. Kudo, G. Deluliis, H. Rahming, H. J. Park, I. Matos, J. Nouws, J. Valdez, J. Lim, K. A. Rose, K. Anastasio, K. Brower, L. Glick, L. Sharma, L. Sewanan, L. Knaggs, M. Minasyan, M. Batsu, M. Kuang, M. Nakahata, M. Linehan, M. H. Askenase, M. Simonov, M. Smolgovsky, N. Sonnert, N. Naushad, P. Vijayakumar, R. Martinello, R. Datta, R. Handoko, S. Bermejo, S. Prophet, S. Bickerton, S. Velazquez, T. Rice, W. Khoury-Hanold, X. Peng, Y. Yang, Y. Cao, Y. Strong, C. dela Cruz, S. F. Farhadian, W. L. Schulz, S. Ma, N. D. Grubaugh, A. I. Ko, A. Iwasaki, A. M. Ring, Diverse functional autoantibodies in patients with COVID-19. *Nature* **595**, 283–288 (2021).
45. M. J. M. Niesen, C. Pawlowski, J. C. O'Horo, D. W. Challener, E. Silvert, G. Donadio, P. J. Lenehan, A. Virk, M. D. Swift, L. L. Speicher, J. E. Gordon, H. L. Geyer, J. D. Halamka, A. J. Venkatakrishnan, V. Soundararajan, A. D. Badley, Surveillance of safety of 3 doses of COVID-19 mRNA vaccination using electronic health records. *JAMA Netw. Open* **5**, e227038 (2022).
46. M. Stoeckius, C. Hafemeister, W. Stephenson, B. Houck-Loomis, P. K. Chattopadhyay, H. Swerdlow, R. Satija, P. Smibert, Simultaneous epitope and transcriptome measurement in single cells. *Nat. Methods* **14**, 865–868 (2017).
47. W. Deng, B. G. Gowen, L. Zhang, L. Wang, S. Lau, A. Iannello, J. Xu, T. L. Rovis, N. Xiong, D. H. Raulet, Antitumor immunity. A shed NKG2D ligand that promotes natural killer cell activation and tumor rejection. *Science* **348**, 136–139 (2015).
48. T. W. Thompson, A. B. Kim, P. J. Li, J. Wang, B. T. Jackson, K. T. H. Huang, L. Zhang, D. H. Raulet, Endothelial cells express NKG2D ligands and desensitize antitumor NK responses. *eLife* **6**, e30881 (2017).
49. M. Büttner, J. Ostner, C. L. Müller, F. J. Theis, B. Schubert, scCODA is a Bayesian model for compositional single-cell data analysis. *Nat. Commun.* **12**, 6876 (2021).
50. R. Altara, Z. Mallat, G. W. Booz, F. A. Zouein, The CXCL10/CXCR3 axis and cardiac inflammation: Implications for immunotherapy to treat infectious and noninfectious diseases of the heart. *J. Immunol. Res.* **2016**, 4396368 (2016).
51. W. W. Hancock, B. Lu, W. Gao, V. Csizmadia, K. Faia, J. A. King, S. T. Smiley, M. Ling, N. P. Gerard, C. Gerard, Requirement of the chemokine receptor CXCR3 for acute allograft rejection. *J. Exp. Med.* **192**, 1515–1520 (2000).
52. I. Komarowska, D. Coe, G. Wang, R. Haas, C. Mauro, M. Kishore, D. Cooper, S. Nadkarni, H. Fu, D. A. Steinbruchel, C. Pitzalis, G. Anderson, P. Bucy, G. Lombardi, R. Breckenridge, F. M. Marelli-Berg, Hepatocyte growth factor receptor c-met instructs T cell cardiotropism and promotes T cell migration to the heart via autocrine chemokine release. *Immunity* **42**, 1087–1099 (2015).

53. F. S. Machado, N. S. Koyama, V. Carregaro, B. R. Ferreira, C. M. Milanezi, M. M. Teixeira, M. A. Rossi, J. S. Silva, CCR5 plays a critical role in the development of myocarditis and host protection in mice infected with Trypanosoma cruzi. *J. Infect. Dis.* **191**, 627–636 (2005).
54. M. Melter, A. Exeni, M. E. J. Reinders, J. C. Fang, G. McMahon, P. Ganz, W. W. Hancock, D. M. Briscoe, Expression of the chemokine receptor CXCR3 and its ligand IP-10 during human cardiac allograft rejection. *Circulation* **104**, 2558–2564 (2001).
55. N. Ngwenyama, A. M. Salvador, F. Velázquez, T. Nevers, A. Levy, M. Aronovitz, A. D. Luster, G. S. Huggins, P. Alcaide, CXCR3 regulates $CD4^+$ T cell cardiotropism in pressure overload-induced cardiac dysfunction. *JCI Insight* **4**, e125527 (2019).
56. E. Roffe, L. I. dos Santos, M. O. Santos, P. M. Henriques, A. Teixeira-Carvalho, O. A. Martins-Filho, M. O. C. Rocha, S. M. Eloi-Santos, R. Correa-Oliveira, L. R. V. Antonelli, Increased frequencies of circulating $CCR5^+$ memory T cells are correlated to chronic chagasic cardiomyopathy progression. *J. Leukoc. Biol.* **106**, 641–652 (2019).
57. V. Szentes, M. Gazdag, I. Szokodi, C. A. Dézsi, The role of CXCR3 and associated chemokines in the development of atherosclerosis and during myocardial infarction. *Front. Immunol.* **9**, 1932 (2018).
58. X. Wang, W. Li, Q. Yue, W. Du, Y. Li, F. Liu, L. Yang, L. Xu, R. Zhao, J. Hu, C-C chemokine receptor 5 signaling contributes to cardiac remodeling and dysfunction under pressure overload. *Mol. Med. Rep.* **23**, 49 (2021).
59. P. S. Arunachalam, M. K. D. Scott, T. Hagan, C. Li, Y. Feng, F. Wimmers, L. Grigoryan, M. Trisal, V. V. Edara, L. Lai, S. E. Chang, A. Feng, S. Dhingra, M. Shah, A. S. Lee, S. Chinthrajah, S. B. Sindher, V. Mallajosyula, F. Gao, N. Sigal, S. Kowli, S. Gupta, K. Pellegrini, G. Tharp, S. Maysel-Auslender, S. Hamilton, H. Aoued, K. Hrusovsky, M. Roskey, S. E. Bosinger, H. T. Maecker, S. D. Boyd, M. M. Davis, P. J. Utz, M. S. Suthar, P. Khatri, K. C. Nadeau, B. Pulendran, Systems vaccinology of the BNT162b2 mRNA vaccine in humans. *Nature* **596**, 410–416 (2021).
60. M. Litviňuková, C. Talavera-López, H. Maatz, D. Reichart, C. L. Worth, E. L. Lindberg, M. Kanda, K. Polanski, M. Heinig, M. Lee, E. R. Nadelmann, K. Roberts, L. Tuck, E. S. Fasouli, D. DeLaughter, B. McDonough, H. Wakimoto, J. M. Gorham, S. Samari, K. T. Mahbubani, K. Saeb-Parsy, G. Patone, J. J. Boyle, H. Zhang, H. Zhang, A. Viveiros, G. Y. Oudit, O. A. Bayraktar, J. G. Seidman, C. E. Seidman, M. Noseda, N. Hubner, S. A. Teichmann, Cells of the adult human heart. *Nature* **588**, 466–472 (2020).
61. M. Moreews, K. le Gouge, S. Khaldi-Plassart, R. Pescarmona, A. L. Mathieu, C. Malcus, S. Djebali, A. Bellomo, O. Dauwalder, M. Perret, M. Villard, E. Chopin, I. Rouvet, F. Vandenesch, C. Dupieux, R. Pouyau, S. Teyssedre, M. Guerder, T. Louazon, A. Moulin-Zinsch, M. Duperril, H. Patural, L. Giovannini-Chami, A. Portefaix, B. Kassai, F. Venet, G. Monneret, C. Lombard, H. Flodrops, J. M. de Guillebon, F. Bajolle, V. Launay, P. Bastard, S. Y. Zhang, V. Dubois, O. Thaunat, J. C. Richard, M. Mezidi, O. Allatif, K. Saker, M. Dreux, L. Abel, J. L. Casanova, J. Marvel, S. Trouillet-Assant, D. Klatzmann, T. Walzer, E. Mariotti-Ferrandiz, E. Javouhey, A. Belot, Polyclonal expansion of TCR Vbeta 21.3$^+$ $CD4^+$ and $CD8^+$T cells is a hallmark of multisystem inflammatory syndrome in children. *Sci. Immunol.* **6**, eabh1516 (2021).
62. R. A. Porritt, L. Paschold, M. N. Rivas, M. H. Cheng, L. M. Yonker, H. Chandnani, M. Lopez, D. Simnica, C. Schultheiß, C. Santiskulvong, J. van Eyk, J. K. McCormick, A. Fasano, I. Bahar, M. Binder, M. Arditi, HLA class I-associated expansion of TRBV11-2 T cells in multisystem inflammatory syndrome in children. *J. Clin. Invest.* **131**, e146614 (2021).
63. A. Ramaswamy, N. N. Brodsky, T. S. Sumida, M. Comi, H. Asashima, K. B. Hoehn, N. Li, Y. Liu, A. Shah, N. G. Ravindra, J. Bishai, A. Khan, W. Lau, B. Sellers, N. Bansal, P. Guerrerio, A. Unterman, V. Habet, A. J. Rice, J. Catanzaro, H. Chandnani, M. Lopez, N. Kaminski, C. S. dela Cruz, J. S. Tsang, Z. Wang, X. Yan, S. H. Kleinstein, D. van Dijk, R. W. Pierce, D. A. Hafler, C. L. Lucas, Immune dysregulation and autoreactivity correlate with disease severity in SARS-CoV-2-associated multisystem inflammatory syndrome in children. *Immunity* **54**, 1083–195.e7 (2021).
64. K. Sacco, R. Castagnoli, S. Vakkilainen, C. Liu, O. M. Delmonte, C. Oguz, I. M. Kaplan, S. Alehashemi, P. D. Burbelo, F. Bhuyan, A. A. de Jesus, K. Dobbs, L. B. Rosen, A. Cheng, E. Shaw, M. S. Vakkilainen, F. Pala, J. Lack, Y. Zhang, D. L. Fink, V. Oikonomou, A. L. Snow, C. L. Dalgard, J. Chen, B. A. Sellers, G. A. Montealegre Sanchez, K. Barron, E. Rey-Jurado, C. Vial, M. C. Poli, A. Licari, D. Montagna, G. L. Marseglia, F. Licciardi, U. Ramenghi, V. Discepolo, A. Lo Vecchio, A. Guarino, E. M. Eisenstein, L. Imberti, A. Sottini, A. Biondi, S. Mató, D. Gerstbacher, M. Truong, M. A. Stack, M. Magliocco, M. Bosticardo, T. Kawai, J. J. Danielson, T. Hulett, M. Askenazi, S. Hu; NIAID Immune Response to COVID Group; Chile MIS-C Group; Pavia Pediatric COVID-19 Group, J. I. Cohen, H. C. Su, D. B. Kuhns, M. S. Lionakis, T. M. Snyder, S. M. Holland, R. Goldbach-Mansky, J. S. Tsang, L. D. Notarangelo, Immunopathological signatures in multisystem inflammatory syndrome in children and pediatric COVID-19. *Nat. Med.* **28**, 1050–1062 (2022).
65. P. B. Narasimhan, P. Marcovecchio, A. A. J. Hamers, C. C. Hedrick, Nonclassical monocytes in health and disease. *Annu. Rev. Immunol.* **37**, 439–456 (2019).
66. G. Thomas, R. Tacke, C. C. Hedrick, R. N. Hanna, Nonclassical patrolling monocyte function in the vasculature. *Arterioscler. Thromb. Vasc. Biol.* **35**, 1306–1316 (2015).
67. W. P. Lafuse, D. J. Wozniak, M. V. S. Rajaman, Role of cardiac macrophages on cardiac inflammation, fibrosis and tissue repair. *Cell* **10**, 51 (2020).
68. C. Xia, Z. Braunstein, A. C. Toomey, J. Zhong, X. Rao, S100 proteins as an important regulator of macrophage inflammation. *Front. Immunol.* **8**, 1908 (2017).
69. A. L. Koenig, I. Shchukina, J. Amrute, P. S. Andhey, K. Zaitsev, L. Lai, G. Bajpai, A. Bredemeyer, G. Smith, C. Jones, E. Terrebonne, S. L. Rentschler, M. N. Artyomov, K. J. Lavine, Single-cell transcriptomics reveals cell-type-specific diversification in human heart failure. *Nat. Cardiovas. Res.* **1**, 263–280 (2022).
70. D. Wendisch, O. Dietrich, T. Mari, S. von Stillfried, I. L. Ibarra, M. Mittermaier, C. Mache, R. L. Chua, R. Knoll, S. Timm, S. Brumhard, T. Krammer, H. Zauber, A. L. Hiller, A. Pascual-Reguant, R. Mothes, R. D. Bülow, J. Schulze, A. M. Leipold, S. Djudjaj, F. Erhard, R. Geffers, F. Pott, J. Kazmierski, J. Radke, P. Pergantis, K. Baßler, C. Conrad, A. C. Aschenbrenner, B. Sawitzki, M. Landthaler, E. Wyler, D. Horst; Deutsche COVID-19 OMICS Initiative (DeCOI), S. Hippenstiel, A. Hocke, F. L. Heppner, A. Uhrig, C. Garcia, F. Machleidt, S. Herold, S. Elezkurtaj, C. Thibeault, M. Witzenrath, C. Cochain, N. Suttorp, C. Drosten, C. Goffinet, F. Kurth, J. L. Schultze, H. Radbruch, M. Ochs, R. Eils, H. Müller-Redetzky, A. E. Hauser, M. D. Luecken, F. J. Theis, C. Conrad, T. Wolff, P. Boor, M. Selbach, A. E. Saliba, L. E. Sander, SARS-CoV-2 infection triggers profibrotic macrophage responses and lung fibrosis. *Cell* **184**, 6243–6261.e27 (2021).
71. M. Nicol, L. Cacoub, M. Baudet, Y. Nahmani, P. Cacoub, A. Cohen-Solal, P. Henry, H. Adle-Biassette, D. Logeart, Delayed acute myocarditis and COVID-19-related multisystem inflammatory syndrome. *ESC Heart Fail* **7**, 4371–4376 (2020).
72. K. M. Vannella, C. Oguz, S. R. Stein, S. Pittaluga, E. Dikoglu, A. Kanwal, S. C. Ramelli, T. Briese, L. Su, X. Wu, M. J. Ramos-Benitez, L. J. Perez-Valencia, A. Babyak, N. R. Cha, J. Y. Chung, K. Ylaya, R. J. Madathil, K. K. Saharia, T. M. Scalea, Q. K. Tran, D. L. Herr, D. E. Kleiner, S. M. Hewitt, L. D. Notarangelo, A. Grazioli, D. S. Chertow, Evidence of SARS-CoV-2-specific T-cell-mediated myocarditis in a MIS-A case. *Front. Immunol.* **12**, 779026 (2021).
73. F. . Ujueta, R. Azimi, M. R. Lozier, R. Poppiti, A. Ciment, Lymphohistocytic myocarditis after Ad26.COV2.S viral vector COVID-19 vaccination. *Int. J. Cardiol. Heart Vasc.* **36**, 100869 (2021).
74. G. Bajpai, C. Schneider, N. Wong, A. Bredemeyer, M. Hulsmans, M. Nahrendorf, S. Epelman, D. Kreisel, Y. Liu, A. Itoh, T. S. Shankar, C. H. Selzman, S. G. Drakos, K. J. Lavine, The human heart contains distinct macrophage subsets with divergent origins and functions. *Nat. Med.* **24**, 1234–1245 (2018).
75. B. Chen, A. Brickshawana, N. G. Frangogiannis, The functional heterogeneity of resident cardiac macrophages in myocardial injury($CCR2^+$ cells promote inflammation, whereas $CCR2^-$ cells protect). *Circ. Res.* **124**, 183–185 (2019).
76. F. Leuschner, G. Courties, P. Dutta, L. J. Mortensen, R. Gorbatov, B. Sena, T. I. Novobrantseva, A. Borodovsky, K. Fitzgerald, V. Koteliansky, Y. Iwamoto, M. Bohlender, S. Meyer, F. Lasitschka, B. Meder, H. A. Katus, C. Lin, P. Libby, F. K. Swirski, D. G. Anderson, R. Weissleder, M. Nahrendorf, Silencing of CCR2 in myocarditis. *Eur. Heart J.* **36**, 1478–1488 (2015).
77. M. Rao, X. Wang, G. Guo, L. Wang, S. Chen, P. Yin, K. Chen, L. Chen, Z. Zhang, X. Chen, X. Hu, S. Hu, J. Song, Resolving the intertwining of inflammation and fibrosis in human heart failure at single-cell level. *Basic Res. Cardiol.* **116**, 55 (2021).
78. R. H. Gantzel, M. B. Kjær, T. L. Laursen, K. Kazankov, J. George, H. J. Møller, H. Grønbæk, Macrophage activation markers, soluble CD163 and mannose receptor, in liver fibrosis. *Front. Med.* **7**, 615599 (2020).
79. M. V. Zanni, M. Awadalla, M. Toribio, J. Robinson, L. A. Stone, D. Cagliero, A. Rokicki, C. P. Mulligan, J. E. Ho, A. M. Neilan, M. J. Siedner, V. A. Triant, T. L. Stanley, L. S. Szczepaniak, M. Jerosch-Herold, M. D. Nelson, T. H. Burdo, T. G. Neilan, Immune correlates of diffuse myocardial fibrosis and diastolic dysfunction among aging women with human immunodeficiency virus. *J. Infect. Dis.* **221**, 1315–1320 (2020).
80. L. Thurner, C. Kessel, N. Fadle, E. Regitz, F. Seidel, I. Kindermann, S. Lohse, I. Kos, C. Tschöpe, P. Kheiroddin, D. Kiblboeck, M.-C. Hoffmann, B. Bette, G. Carbon, O. Cetin, K.-D. Preuss, K. Christofyllakis, J. T. Bittenbring, T. Pickardt, Y. Fischer, H. Thiele, S. Baldus, K. Stangl, S. Steiner, F. Gietzen, S. Kerber, T. Deneke, S. Jellinghaus, A. Linke, K. Ibrahim, U. Grabmaier, S. Massberg, C. Thilo, S. Greulich, M. Gawaz, E. Mayatepek, L. Meyer-Dobkowitz, M. Kindermann, E. Birk, M. Birk, M. Lainscak, D. Foell, P. M. Lepper, R. Bals, M. Krawczyk, D. Mevorach, T. Hasin, A. Keren, M. Kabesch, H. Abdul-Khaliq, S. Smola, M. Bewarder, B. Thurner, M. Böhm, J. Pfeifer, K. Klingel, IL-1RA antibodies in myocarditis after SARS-CoV-2 vaccination. *N. Engl. J. Med.* **387**, 1524–1527 (2022).
81. N. Chaudhary, D. Weissman, K. A. Whitehead, mRNA vaccines for infectious diseases: Principles, delivery and clinical translation. *Nat. Rev. Drug Discov.* **20**, 817–838 (2021).
82. X. Hou, T. Zaks, R. Langer, Y. Dong, Lipid nanoparticles for mRNA delivery. *Nat. Rev. Mater.* **6**, 1078–1094 (2021).
83. S. Al-Kindi, D. A. Zidar, COVID-lateral damage: Cardiovascular manifestations of SARS-CoV-2 infection. *Transl. Res.* **241**, 25–40 (2022).

84. O. Blagova, N. Varionchik, V. Zaidenov, P. Savina, N. Sarkisova, Anti-heart antibodies levels and their correlation with clinical symptoms and outcomes in patients with confirmed or suspected diagnosis COVID-19. *Eur. J. Immunol.* **51**, 893–902 (2021).
85. M. E. Laino, A. Ammirabile, F. Motta, M. De Santis, V. Savevski, M. Francone, A. Chiti, L. Mannelli, C. Selmi, L. Monti, Advanced imaging supports the mechanistic role of autoimmunity and plaque rupture in COVID-19 heart involvement. *Clin. Rev. Allergy Immunol.* **64**, 75–89 (2023).
86. J. R. Jaycox, C. Lucas, I. Yildirim, Y. Dai, E. Y. Wang, V. Monteiro, S. Lord, J. Carlin, M. Kita, J. H. Buckner, S. Ma, M. Campbell, A. Ko, S. Omer, C. L. Lucas, C. Speake, A. Iwasaki, A. M. Ring, SARS-CoV-2 mRNA vaccines decouple anti-viral immunity from humoral autoimmunity. *Nat. Commun.* **14**, 1299 (2023).
87. W. J. Murphy, D. L. Longo, A possible role for anti-idiotype antibodies in SARS-CoV-2 infection and vaccination. *N. Engl. J. Med.* **386**, 394–396 (2022).
88. P. Spear, M. R. Wu, M. L. Sentman, C. L. Sentman, NKG2D ligands as therapeutic targets. *Cancer Immun.* **13**, 8 (2013).
89. M. Babic, C. Dimitropoulos, Q. Hammer, C. Stehle, F. Heinrich, A. Sarsenbayeva, A. Eisele, P. Durek, M.-F. Mashreghi, B. Lisnic, J. Van Snick, M. Löhning, S. Fillatreau, D. R. Withers, N. Gagliani, S. Huber, R. A. Flavell, B. Polic, C. Romagnani, NK cell receptor NKG2D enforces proinflammatory features and pathogenicity of Th1 and Th17 cells. *J. Exp. Med.* **217**, e20190133 (2020).
90. M. Champsaur, L. L. Lanier, Effect of NKG2D ligand expression on host immune responses. *Immunol. Rev.* **235**, 267–285 (2010).
91. M. Karimi, T. M. Cao, J. A. Baker, M. R. Verneris, L. Soares, R. S. Negrin, Silencing human NKG2D, DAP10, and DAP12 reduces cytotoxicity of activated CD8+ T cells and NK cells. *J. Immunol.* **175**, 7819–7828 (2005).
92. K. Maasho, J. Opoku-Anane, A. I. Marusina, J. E. Coligan, F. Borrego, Cutting edge: NKG2D is a costimulatory receptor for human naive $CD8^+$ T cells. *J. Immunol.* **174**, 4480–4484 (2005).
93. K. Matsumoto, M. Obana, A. Kobayashi, M. Kihara, G. Shioi, S. Miyagawa, M. Maeda, Y. Sakata, H. Nakayama, Y. Sawa, Y. Fujio, Blockade of NKG2D/NKG2D ligand interaction attenuated cardiac remodelling after myocardial infarction. *Cardiovasc. Res.* **115**, 765–775 (2019).
94. R. Molfetta, L. Quatrini, B. Zitti, C. Capuano, R. Galandrini, A. Santoni, R. Paolini, Regulation of NKG2D expression and signaling by endocytosis. *Trends Immunol.* **37**, 790–802 (2016).
95. B. Suárez-Alvarez, A. López-Vázquez, J. M. Baltar, F. Ortega, C. López-Larrea, Potential role of NKG2D and its ligands in organ transplantation: New target for immunointervention. *Am. J. Transplant.* **9**, 251–257 (2009).
96. F. M. Wensveen, V. Jelenˇić, B. Polić, NKG2D: A master regulator of immune cell responsiveness. *Front. Immunol.* **9**, (2018).
97. W. E. Carson, J. G. Giri, M. J. Lindemann, M. L. Linett, M. Ahdieh, R. Paxton, D. Anderson, J. Eisenmann, K. Grabstein, M. A. Caligiuri, Interleukin (IL) 15 is a novel cytokine that activates human natural killer cells via components of the IL-2 receptor. *J. Exp. Med.* **180**, 1395–1403 (1994).
98. J. Kim, D.-Y. Chang, H. W. Lee, H. Lee, J. H. Kim, P. S. Sung, K. H. Kim, S.-H. Hong, W. Kang, J. Lee, S. Y. Shin, H. T. Yu, S. You, Y. S. Choi, I. Oh, D. H. Lee, D. H. Lee, M. K. Jung, K.-S. Suh, S. Hwang, W. Kim, S.-H. Park, H. J. Kim, E.-C. Shin, Innate-like cytotoxic function of bystander-activated $CD8^+$ T cells is associated with liver injury in acute hepatitis A. *Immunity* **48**, 161–173 (2018).
99. T. A. Waldmann, Y. Tagaya, The multifaceted regulation of interleukin-15 expression and the role of this cytokine in NK cell differentiation and host response to intracellular pathogens. *Annu. Rev. Immunol.* **17**, 19–49 (1999).
100. S.-A. Younes, M. L. Freeman, J. C. Mudd, C. L. Shive, A. Reynaldi, S. Panigrahi, J. D. Estes, C. Deleage, C. Lucero, J. Anderson, T. W. Schacker, M. P. Davenport, J. M. M. Cune, P. W. Hunt, S. A. Lee, S. Serrano-Villar, R. L. Debernardo, J. M. Jacobson, D. H. Canaday, R.-P. Sekaly, B. Rodriguez, S. F. Sieg, M. M. Lederman, IL-15 promotes activation and expansion of $CD8^+$ T cells in HIV-1 infection. *J. Clin. Invest.* **126**, 2745–2756 (2016).
101. M. Barton, Y. Finkelstein, M. A. Opavsky, S. Ito, T. Ho, L. E. Ford-Jones, G. Taylor, L. Benson, R. Gold, Eosinophilic myocarditis temporally associated with conjugate meningococcal C and hepatitis B vaccines in children. *Pediatr. Infect. Dis. J.* **27**, 831–835 (2008).
102. J. G. Murphy, R. S. Wright, G. K. Bruce, L. M. Baddour, M. A. Farrell, W. D. Edwards, H. . Kita, L. T. Cooper, Eosinophilic-lymphocytic myocarditis after smallpox vaccination. *Lancet* **362**, 1378–1380 (2003).
103. H. Yamamoto, T. Hashimoto, K. Ohta-Ogo, H. Ishibashi-Ueda, K. Imanaka-Yoshida, M. Hiroe, T. Yokochi, A case of biopsy-proven eosinophilic myocarditis related to tetanus toxoid immunization. *Cardiovasc. Pathol.* **37**, 54–57 (2018).
104. G. Georgiopoulos, S. Figliozzi, F. Sanguineti, G. D. Aquaro, G. di Bella, K. Stamatelopoulos, A. Chiribiri, J. Garot, P. G. Masci, T. F. Ismail, Prognostic impact of late gadolinium enhancement by cardiovascular magnetic resonance in myocarditis: A systematic review and meta-analysis. *Circ. Cardiovasc. Imaging* **14**, e011492 (2021).
105. S. Kuruvilla, N. Adenaw, A. B. Katwal, M. J. Lipinski, C. M. Kramer, M. Salerno, Late gadolinium enhancement on cardiac magnetic resonance predicts adverse cardiovascular outcomes in nonischemic cardiomyopathy: A systematic review and meta-analysis. *Circ. Cardiovasc. Imaging* **7**, 250–258 (2014).
106. A. Nojiri, K. Hongo, M. Kawai, K. Komukai, T. Sakuma, I. Taniguchi, M. Yoshimura, Scoring of late gadolinium enhancement in cardiac magnetic resonance imaging can predict cardiac events in patients with hypertrophic cardiomyopathy. *J. Cardiol.* **58**, 253–260 (2011).
107. M. Fertin, G. Lemesle, A. Turkieh, O. Beseme, M. Chwastyniak, P. Amouyel, C. Bauters, F. Pinet, Serum MMP-8: A novel indicator of left ventricular remodeling and cardiac outcome in patients after acute myocardial infarction. *PLOS ONE* **8**, e71280 (2013).
108. G. V. Halade, Y. F. Jin, M. L. Lindsey, Matrix metalloproteinase (MMP)-9: A proximal biomarker for cardiac remodeling and a distal biomarker for inflammation. *Pharmacol. Ther.* **139**, 32–40 (2013).
109. J. Hansson, R. S. Vasan, J. Ärnlöv, E. Ingelsson, L. Lind, A. Larsson, K. Michaëlsson, J. Sundström, Biomarkers of extracellular matrix metabolism (MMP-9 and TIMP-1) and risk of stroke, myocardial infarction, and cause-specific mortality: Cohort study. *PLOS ONE* **6**, e16185 (2011).
110. R. P. Iyer, M. Jung, M. L. Lindsey, MMP-9 signaling in the left ventricle following myocardial infarction. *Am. J. Physiol. Heart Circ. Physiol.* **311**, H190–H198 (2016).
111. F. Shahid, G. Y. H. Lip, E. Shantsila, Role of monocytes in heart failure and atrial fibrillation. *J. Am. Heart Assoc.* **7**, e007849 (2018).
112. C. Schwab, L. M. Domke, L. Hartmann, A. Stenzinger, T. Longerich, P. Schirmacher, Autopsy-based histopathological characterization of myocarditis after anti-SARS-CoV-2-vaccination. *Clin. Res. Cardiol.* **112**, 431–440 (2023).
113. C. Bergamaschi, E. Terpos, M. Rosati, M. Angel, J. Bear, D. Stellas, S. Karaliota, F. Apostolakou, T. Bagratuni, D. Patseas, S. Gumeni, I. P. Trougakos, M. A. Dimopoulos, B. K. Felber, B. K. Pavlakis, Systemic IL-15, IFN-γ, and IP-10/CXCL10 signature associated with effective immune response to SARS-CoV-2 in BNT162b2 mRNA vaccine recipients. *Cell Rep.* **36**, 109504 (2021).
114. N. Grabie, A. H. Lichtman, R. Padera, T cell checkpoint regulators in the heart. *Cardiovasc. Res.* **115**, 869–877 (2019).
115. J. K. Hu, T. Kagari, J. M. Clingan, M. Matloubian, Expression of chemokine receptor CXCR3 on T cells affects the balance between effector and memory CD8 T-cell generation. *Proc. Natl. Acad. Sci. U.S.A.* **108**, E118–E127 (2011).
116. J. E. Kohlmeier, W. W. Reiley, G. Perona-Wright, M. L. Freeman, E. J. Yager, L. M. Connor, E. L. Brincks, T. Cookenham, A. D. Roberts, C. E. Burkum, S. Sell, G. M. Winslow, M. A. Blackman, M. Mohrs, D. L. Woodland, Inflammatory chemokine receptors regulate CD8(+) T cell contraction and memory generation following infection. *J. Exp. Med.* **208**, 1621–1634 (2011).
117. M. Kurachi, J. Kurachi, F. Suenaga, T. Tsukui, J. Abe, S. Ueha, M. Tomura, K. Sugihara, S. Takamura, K. Kakimi, K. Matsushima, Chemokine receptor CXCR3 facilitates $CD8^+$ T cell differentiation into short-lived effector cells leading to memory degeneration. *J. Exp. Med.* **208**, 1605–1620 (2011).
118. R. Sparks, W. W. Lau, C. Liu, K. L. Han, K. L. Vrindten, G. Sun, M. Cox, S. F. Andrews, N. Bansal, L. E. Failla, J. Manischewitz, G. Grubbs, L. R. King, G. Koroleva, S. Leimenstoll, L. Snow; Staff OPC, J. Chen, J. Tang, A. Mukherjee, B. A. Sellers, R. Apps, A. B. McDermott, A. J. Martins, E. M. Bloch, H. Golding, S. Khurana, J. S. Tsang, Influenza vaccination reveals sex dimorphic imprints of prior mild COVID-19. *Nature* **614**, 752–761 (2023).
119. J. Domínguez-Andrés, M. G. Netea, The specifics of innate immune memory. *Science* **368**, 1052–1053 (2020).
120. A. Mantovani, M. G. Netea, Trained innate immunity, epigenetics, and Covid-19. *N. Engl. J. Med.* **383**, 1078–1080 (2020).
121. A. M. Mujal, R. B. Delconte, J. C. Sun, Natural killer cells: From innate to adaptive features. *Annu. Rev. Immunol.* **39**, 417–447 (2021).
122. M. G. Netea, J. Domínguez-Andrés, L. B. Barreiro, T. Chavakis, M. Divangahi, E. Fuchs, L. A. B. Joosten, J. W. M. van der Meer, M. M. Mhlanga, W. J. M. Mulder, N. P. Riksen, A. Schlitzer, J. L. Schultze, C. S. Benn, J. C. Sun, R. J. Xavier, E. Latz, Defining trained immunity and its role in health and disease. *Nat. Rev. Immunol.* **20**, 375–388 (2020).
123. M.-G. Alameh, I. Tombácz, E. Bettini, K. Lederer, C. Sittplangkoon, J. R. Wilmore, B. T. Gaudette, O. Y. Soliman, M. Pine, P. Hicks, T. B. Manzoni, J. J. Knox, J. L. Johnson, D. Laczkó, H. Muramatsu, B. Davis, W. Meng, A. M. Rosenfeld, S. Strohmeier, P. J. C. Lin, B. L. Mui, Y. K. Tam, K. Karikó, A. Jacquet, F. Krammer, P. Bates, M. P. Cancro, D. Weissman, E. T. Luning Prak, D. Allman, M. Locci, N. Pardi, Lipid nanoparticles enhance the efficacy of mRNA and protein subunit vaccines by inducing robust T follicular helper cell and humoral responses. *Immunity* **54**, 2877–92.e7 (2021).
124. S. Tahtinen, A.-J. Tong, P. Himmels, J. Oh, A. Paler-Martinez, L. Kim, S. Wichner, Y. Oei, M. J. McCarron, E. C. Freund, Z. A. Amir, C. C. de la Cruz, B. Haley, C. Blanchette, J. M. Schartner, W. Ye, M. Yadav, U. Sahin, L. Delamarre, I. Mellman, IL-1 and IL-1ra are key

regulators of the inflammatory response to RNA vaccines. *Nat. Immunol.* **23**, 532–542 (2022).
125. V. Kytö, J. Sipilä, P. Rautava, The effects of gender and age on occurrence of clinically suspected myocarditis in adulthood. *Heart* **99**, 1681–1684 (2013).
126. V. Kyto, J. Sipila, P. Rautava, Gender differences in myocarditis: A nationwide study in Finland. *Eur. Heart J.* **34**, 3505 (2013).
127. V. Kytö, J. Sipilä, P. Rautava, Clinical profile and influences on outcomes in patients hospitalized for acute pericarditis. *Circulation* **130**, 1601–1606 (2014).
128. M. Laufer-Perl, O. Havakuk, Y. Shacham, A. Steinvil, S. Letourneau-Shesaf, E. Chorin, G. Keren, Y. Arbel, Sex-based differences in prevalence and clinical presentation among pericarditis and myopericarditis patients. *Am. J. Emerg. Med.* **35**, 201–205 (2017).
129. K. Ozierański, A. Tymińska, A. Skwarek, M. Kruk, B. Koń, J. Biliński, G. Opolski, M. Grabowski, Sex differences in incidence, clinical characteristics and outcomes in children and young adults hospitalized for clinically suspected myocarditis in the last ten years-data from the MYO-PL nationwide database. *J. Clin. Med.* **10**, 5502 (2021).
130. D. Patriki, J. Kottwitz, J. Berg, U. Landmesser, T. F. Lüscher, B. Heidecker, Clinical presentation and laboratory findings in men versus women with myocarditis. *J. Womens Health* **29**, 193–199 (2020).
131. Z. Shah, M. Mohammed, V. Vuddanda, M. W. Ansari, R. Masoomi, K. Gupta, National trends, gender, management, and outcomes of patients hospitalized for myocarditis. *Am. J. Cardiol.* **124**, 131–136 (2019).
132. A. Younis, W. Mulla, S. Matetzky, E. Masalha, Y. Afel, A. Fardman, O. Goitein, M. Arad, I. Mazin, R. Beigel, Sex-based differences in characteristics and in-hospital outcomes among patients with diagnosed acute myocarditis. *Am. J. Cardiol.* **125**, 1694–1699 (2020).
133. M. L. Barcena, S. Jeuthe, M. H. Niehues, S. Pozdniakova, N. Haritonow, A. A. Kühl, D. R. Messroghli, V. Regitz-Zagrosek, Sex-specific differences of the inflammatory state in experimental autoimmune myocarditis. *Front. Immunol.* **12**, 686384 (2021).
134. M. S. Cocker, H. Abdel-Aty, O. Strohm, M. G. Friedrich, Age and gender effects on the extent of myocardial involvement in acute myocarditis: A cardiovascular magnetic resonance study. *Heart* **95**, 1925–1930 (2009).
135. A. Bignucolo, L. Scarabel, S. Mezzalira, J. Polesel, E. Cecchin, G. Toffoli, Sex disparities in efficacy in COVID-19 vaccines: A systematic review and meta-analysis. *Vaccines* **9**, 825 (2021).
136. A. Jensen, M. Stromme, S. Moyassari, A. S. Chadha, M. C. Tartaglia, C. Szoeke, M. T. Ferretti, COVID-19 vaccines: Considering sex differences in efficacy and safety. *Contemp. Clin. Trials* **115**, 106700 (2022).
137. Z. Al-Aly, Y. Xie, B. Bowe, High-dimensional characterization of post-acute sequelae of COVID-19. *Nature* **594**, 259–264 (2021).
138. P. N. Jone, A. John, M. E. Oster, K. Allen, A. H. Tremoulet, E. V. Saarel, L. M. Lambert, S. D. Miyamoto, S. D. de Ferranti, SARS-CoV-2 infection and associated cardiovascular manifestations and complications in children and young adults: A scientific statement from the american heart association. *Circulation* **145**, e1037–e1052 (2022).
139. T. Patel, M. Kelleman, Z. West, A. Peter, M. Dove, A. Butto, M. E. Oster, Comparison of multisystem inflammatory syndrome in children-related myocarditis, classic viral myocarditis, and COVID-19 vaccine-related myocarditis in children. *J. Am. Heart Assoc.* **11**, e024393 (2022).
140. Y. Xie, E. Xu, B. Bowe, Z. Al-Aly, Long-term cardiovascular outcomes of COVID-19. *Nat. Med.* **28**, 583–590 (2022).
141. F. Amanat, D. Stadlbauer, S. Strohmeier, T. H. O. Nguyen, V. Chromikova, M. McMahon, K. Jiang, G. Asthagiri Arunkumar, D. Jurczyszak, J. Polanco, M. Bermudez-Gonzalez, G. Kleiner, T. Aydillo, L. Miorin, D. Fierer, L. Amarilis Lugo, E. Milunka Kojic, J. Stoever, S. T. H. Liu, C. Cunningham-Rundles, P. L. Felgner, T. Moran, A. Garcia-Sastre, D. Caplivski, A. Cheng, K. Kedzierska, O. Vapalahti, J. M. Hepojoki, V. Simon, F. Krammer, A serological assay to detect SARS-CoV-2 seroconversion in humans. *Nat. Med.* **26**, 1033–1036 (2020).
142. C. Lucas, P. Wong, J. Klein, T. B. R. Castro, J. Silva, M. Sundaram, M. K. Ellingson, T. Mao, J. E. Oh, B. Israelow, T. Takahashi, M. Tokuyama, P. Lu, A. Venkataraman, A. Park, S. Mohanty, H. Wang, A. L. Wyllie, C. B. F. Vogels, R. Earnest, S. Lapidus, I. M. Ott, A. J. Moore, M. C. Muenker, J. B. Fournier, M. Campbell, C. D. Odio, A. Casanovas-Massana, I. T. Yale, R. Herbst, A. C. Shaw, R. Medzhitov, W. L. Schulz, N. D. Grubaugh, C. Dela Cruz, S. Farhadian, A. I. Ko, S. B. Omer, A. Iwasaki, Longitudinal analyses reveal immunological misfiring in severe COVID-19. *Nature* **584**, 463–469 (2020).
143. Gene OntologyConsortium, The Gene Ontology resource: Enriching a GOld mine. *Nucleic Acids Res.* **49**, D325–D334 (2021).
144. M. Ashburner, C. A. Ball, J. A. Blake, D. Botstein, H. Butler, J. M. Cherry, A. P. Davis, K. Dolinski, S. S. Dwight, J. T. Eppig, M. A. Harris, D. P. Hill, L. Issel-Tarver, A. Kasarskis, S. Lewis, J. C. Matese, J. E. Richardson, M. Ringwald, G. M. Rubin, G. Sherlock, Gene ontology: Tool for the unification of biology. The Gene Ontology Consortium. *Nat. Genet.* **25**, 25–29 (2000).
145. G. X. Zheng, J. M. Terry, P. Belgrader, P. Ryvkin, Z. W. Bent, R. Wilson, S. B. Ziraldo, T. D. Wheeler, G. P. McDermott, J. Zhu, M. T. Gregory, J. Shuga, L. Montesclaros, J. G. Underwood, D. A. Masquelier, S. Y. Nishimura, M. Schnall-Levin, P. W. Wyatt, C. M. Hindson, R. Bharadwaj, A. Wong, K. D. Ness, L. W. Beppu, H. J. Deeg, C. McFarland, K. R. Loeb, W. J. Valente, N. G. Ericson, E. A. Stevens, J. P. Radich, T. S. Mikkelsen, B. J. Hindson, J. H. Bielas, Massively parallel digital transcriptional profiling of single cells. *Nat. Commun.* **8**, 14049 (2017).
146. R. Lopez, J. Regier, M. B. Cole, M. I. Jordan, N. Yosef, Deep generative modeling for single-cell transcriptomics. *Nat. Methods* **15**, 1053–1058 (2018).
147. A. Butler, P. Hoffman, P. Smibert, E. Papalexi, R. Satija, Integrating single-cell transcriptomic data across different conditions, technologies, and species. *Nat. Biotechnol.* **36**, 411–420 (2018).
148. S. L. Wolock, R. Lopez, A. M. Klein, Scrublet: Computational identification of cell doublets in single-cell transcriptomic data. *Cell Syst.* **8**, 281–291.e9 (2019).
149. F. A. Wolf, P. Angerer, F. J. Theis, SCANPY: Large-scale single-cell gene expression data analysis. *Genome Biol.* **19**, 15 (2018).
150. C. S. Smillie, M. Biton, J. Ordovas-Montanes, K. M. Sullivan, G. Burgin, D. B. Graham, R. H. Herbst, N. Rogel, M. Slyper, J. Waldman, M. Sud, E. Andrews, G. Velonias, A. L. Haber, K. Jagadeesh, S. Vickovic, J. Yao, C. Stevens, D. Dionne, L. T. Nguyen, A. C. Villani, M. Hofree, E. A. Creasey, H. Huang, O. Rozenblatt-Rosen, J. J. Garber, H. Khalili, A. N. Desch, M. J. Daly, A. N. Ananthakrishnan, A. K. Shalek, R. J. Xavier, A. Regev, Intra- and inter-cellular rewiring of the human colon during ulcerative colitis. *Cell* **178**, 714–730.e22 (2019).
151. M. E. Ritchie, B. Phipson, D. Wu, Y. Hu, C. W. Law, W. Shi, G. K. Smyth, limma powers differential expression analyses for RNA-sequencing and microarray studies. *Nucleic Acids Res.* **43**, e47 (2015).
152. M. D. Robinson, D. J. McCarthy, G. K. Smyth, edgeR: A bioconductor package for differential expression analysis of digital gene expression data. *Bioinformatics* **26**, 139–140 (2010).
153. N. T. Gupta, J. A. Vander Heiden, M. Uduman, D. Gadala-Maria, G. Yaari, S. H. Kleinstein, Change-O: A toolkit for analyzing large-scale B cell immunoglobulin repertoire sequencing data. *Bioinformatics* **31**, 3356–3358 (2015).
154. N. Borcherding, N. L. Bormann, G. Kraus, scRepertoire: An R-based toolkit for single-cell immune receptor analysis. *F1000Res* **9**, 47 (2020).

Acknowledgments: We thank the patients and their families for participation in research and all clinical care staff for their contributions. We also thank A. Zaleski, T. Murray, A. Rice, J. Wang, K. Hoehn, X. Yan, N. Li, and the Yale Center for Genome Analysis (YCGA) staff for their contributions. **Funding:** C.L.L. acknowledges funding from NIAID/NIH (R21AI144315-S1) and Yale University. A.B. is supported by the NIGMS/NIH Medical Scientist Training Grant (T32GM136651) and the Paul and Daisy Soros Fellowship. J.K. is supported by the NIGMS/NIH Medical Scientist Training Grant (T32GM136651). N.N.B. acknowledges funding from the Yale Center for Clinical Investigation and PCCTSDP/NICHD/NIH. T.S.S. acknowledges funding from Race to Erase MS Young Investigator award. I.Y. acknowledges funding from NIAID/NIH, Centers for Disease Control, and Bill and Melinda Gates Foundation. A.I. acknowledges funding from the Howard Hughes Medical Institute. C.R.O. acknowledges funding from NIAID/NIH (K23AI159518). D.B. acknowledges funding from NIAID/NIH (R01HD108467). The contents of this work are solely the responsibility of the authors and do not necessarily represent the official views of the NIH. **Author contributions:** A.B., J.K., A.M.R., S.B.O., A.I., I.Y., and C.L.L. conceptualized, designed, and oversaw the research. N.N.B., H.S., V.H., M.C., A.K., D.B., C.R.O., J.S., E.K.H., and I.Y. coordinated clinical samples and data. A.B., J.K., A.R., J.R.J., K.M.J., T.S.S., M.P.-H., V.M., and C.L. performed experiments, analyzed data, and prepared figures. A.B., J.K., A.I., I.Y., and C.L.L. wrote the manuscript with input and review from all authors. **Competing interests:** C.L.L. reported an unrelated advisory/consulting role for Pharming Healthcare Inc. and unrelated funding to her institution from Ono Pharma. I.Y. reported being a member of the NIAID/COVPN mRNA-1273 Study Group; has received funding to her institution to conduct clinical research from Pfizer and Moderna outside the submitted work; and has an unrelated advisory/consulting role for Sanofi Pasteur and Merck. A.I. cofounded and consults for RIGImmune, Xanadu Bio, and PanV; consults for Paratus Sciences and InvisiShield Technologies; and is a member of the Board of Directors of Roche Holding Ltd. A.M.R. is an inventor of a patent describing the REAP technology and is the founder of and holds equity in Seranova Bio, the commercial licensee of this patent. D.B. is the founder of Lab11 Therapeutics. S.B.O. serves on various WHO advisory committees and on the boards of Gavi, the Vaccine Alliance, and Sabin Vaccine Institute. **Data and materials availability:** The scRNA-seq data from the patients with myopericarditis and VCs used in this study are available through the Gene Expression Omnibus (GEO) database under accession number GSE230227. Previously published single-cell data (*63*) from pediatric HD controls and patients with MIS-C used in this study can be found at GEO under accession number GSE166489. All other data needed to evaluate the conclusions in the paper are present in the paper or the Supplementary Materials. Scripts used for analysis in this study followed standard code as detailed in Materials and Methods and are available upon request.

Submitted 26 February 2023
Accepted 19 April 2023
Published 5 May 2023
10.1126/sciimmunol.adh3455